

# Parametric Investigations on a Prismatic Lithium-Ion Battery Pack with a Mini-Channel Cold Plate for Effective Thermal Management

SR. Shravan Kumar<sup>1</sup>; M. Ramu<sup>2</sup>; G. Amba Prasad Rao<sup>3\*</sup>

<sup>3</sup>Professor

<sup>1,2,3</sup> Department of Mechanical Engineering, National Institute of Technology Warangal, Warangal-506 004, Telangana, India

Corresponding Author: G. Amba Prasad Rao<sup>3\*</sup>

Publication Date: 2025/06/23

**Abstract:** Lithium-ion batteries have become a prominent ultimate choice due to their inherent advantages. However, their performance is susceptible, especially at high temperatures arising out of fast charging and high discharge rates. A good battery thermal management to overcome thermal runaway due to the temperature sensitivity of power batteries. Liquid cooling with water as a coolant has emerged as an integral part of electric vehicle-related research. For effective liquid cooling, the use of min-channel cold plates is explored but with complicated circuits of liquid flow. Present work deals with, two simple designs- Design 1 and Design 2, and their efficacy has been tried out by varying numbers of channels, cross-section of channels, profile of channels and inlet mass flow rate of coolant under 3C and 5C discharge rates for a prismatic Lithium-ion battery pack. A systematic and extensive simulations are performed, using ANSYS FLUENT 2023 R1, maintaining uniform initial boundary conditions of ambient pressure and temperature, 300 K. To begin with, simulations are performed on a single cell and extended up to battery pack with and without mini-channel cold plate. It is observed that Design 2 yielded better thermal performance in terms of lowest peak temperature and lowest temperature difference across the cells with marginally high-pressure drop for zig-zag profile compared to straight channels with a temperature difference of about 12 K. The simulation study well predicted the thermal behavior of single cell, mini-channel cold plate and battery pack with two different designs.

**Keywords:** Batteries, Thermal Runaway, Designs, Channels, Mass Flow Rate.

**How to Cite:** SR. Shravan Kumar; M. Ramu; G. Amba Prasad Rao (2025). Parametric Investigations on a Prismatic Lithium-Ion Battery Pack with a Mini-Channel Cold Plate for Effective Thermal Management. *International Journal of Innovative Science and Research Technology*, 10(6), 1430-1453.

<https://doi.org/10.38124/ijisrt/25jun940>

## Abbreviations

BEV	Battery-powered electric vehicle
BTMS	Battery Thermal Management System
EV	Electric Vehicle
HEV	Hybrid Electric Vehicle
ICEV	Internal Combustion Engine Vehicle
LIB	Lithium-ion Battery
MCP	Mini-channel Cold Plate
PCM	Phase Change Material

DoD	Depth of discharge
D	Hydraulic diameter, mm
h	Convective heat transfer coefficient, $W.m^{-2}K^{-1}$
$Q_g$	Heat generated in the battery, $W.m^{-3}$
$T_{max}$	Peak temperature, K
$C_p$	Specific heat capacity, $J.kg^{-1}K^{-1}$
T	Temperature, K
K	Thermal conductivity, $W.m^{-1}K^{-1}$
P	Pressure, Pa
A	Amplitude
$\rho$	Density, $kg.m^{-3}$
$\mu$	Dynamic viscosity, $kg.m^{-1}.s^{-1}$ .

## I. INTRODUCTION

The automotive industry dominated by fossil fuel-run ICEVs undoubtedly brought huge growth in the economy by giving space for other industries to grow, but it also brought twin problems of fuel crisis and harmful exhaust emissions. Many efforts have been made to overcome these issues with the introduction of alternative fuels, alternative combustion concepts, exhaust gas after-treatment devices, stringent emission norms, etc.<sup>1,2</sup>. No doubt, these developments have reduced the problems to a certain extent, but with an increase in the automotive population, not much difference is seen. Of late, alternative prime movers, especially pure electric vehicles, have been increasing in the market and found advantageous with their near-zero local pollution. These EVs and its different variants are run with batteries and electric motors with Lithium-ion batteries serving the majority of energy purposes even though there are other rechargeable batteries available<sup>3</sup>.

The LIBs have been the most sought after due to their high energy density and long cycle life; however, they are prone to thermal runaway and associated catastrophic issues arising mainly due to high temperature as they run under different ambient and operating conditions<sup>4</sup>. Large-scale promotion of

EVs would not only reduce local emissions but also encourage the utilization of renewable energy sources, thereby meeting the mandate of UNO's SDGs.

### ➤ *Lithium-Ion Batteries and Its Characteristics*

A Lithium-ion cell is essentially an electrochemical conversion device consisting of a cathode, anode, separator current collectors and electrolyte. Lithium ions travel from the anode to the cathode during discharging through the electrolyte, creating a way for the flow of electrons, thereby generating electric current. During charging, the cathode releases lithium ions, and then the lithium ions will go back to the anode. Since the lithium ions are exchanged between the cathode and anode, the lithium-ion batteries back and forth are

thus regarded as "*Rocking Chair Battery*". The LIB basic chemistry and different materials used for anode, cathode, separator and electrolyte and their specific properties are well documented<sup>5,6</sup>. There are works related to a review of efforts done on the quick charging of electric vehicles<sup>7</sup>. To understand heat generation along with working, various electric circuit models for batteries have been reviewed<sup>8</sup>.

### ➤ *Effect of Operating Temperature on the Performance of the Battery*

Though the LIBs have great potential as energy source for EVs, but they are very sensitive to temperature of working and environment conditions. At high temperatures arise out of ambient or working heat generation during charging and fast discharging, high discharge rates due to varying operating conditions batteries experience occur<sup>9-12</sup>.

The effect of non-uniform temperature among cells in a battery pack has been investigated. It is observed that when the temperature difference is more than 5 °C, the battery's capacity is reduced by 2%. Therefore, in order to ensure the safety and optimal performance of the electric vehicles which are powered by LIBs, the  $T_{max}$  of LIBs should be maintained in the range of 15 °C to 40 °C with  $\Delta T_{max}$  inside the battery pack less than 5°C<sup>13</sup>. To maintain such values, an effective BTMS needs to be integrated into the electric vehicle so that it can regulate the temperature by dissipating away the heat generated during discharge and also can preheat the battery whenever needed.

The LIB chemistries, details of its components and causes such as thermal abuse, electrical abuse and mechanical abuse, and associated catastrophic effects of thermal runaway have been understood and inferred that hence the performance of LIBs is optimum within a narrow range of temperature<sup>5</sup>. At low temperatures, the rate of chemical reactions will be slower resulting in a decrease in the production of electric power. With the decrease in temperature, electrode materials will contract, resulting in a slowing down of ion movements. At too low temperatures, the electrodes will stop generating

current flow, which results in a decrease in power output<sup>12</sup>. At high temperatures of battery (> 40°C), battery side reactions will be intensified, resulting in capacity loss and a decrease in the life cycle. Also, at Temperatures exceeding 70°C, serious issues like thermal runaway set in take place, resulting in fire or explosion accidents of EVs<sup>14</sup>.

#### ➤ *Battery Thermal Management System (BTMS)*

BTMS can be regarded as the brain of a battery pack. Several battery cells can be arranged in a battery pack in series, parallel, or a combination of both series and parallel, depending upon the requirement<sup>15</sup>. A proper BTMS needs to be designed to maintain the temperature of the LIBs in the optimal range of 15°C to 40°C with a temperature difference of less than 5°C. Broadly, the BTMS is classified as internal and external, further the external systems are divided into active passive and hybrid systems<sup>16,17</sup>.

#### ➤ *Active BTMS by Using Mini-Channel Cold Plates*

Though the BTMS works initially started with natural/forced air circulation, due to low dissipation rates, liquid cooling with water has become dominant in the research. Both air and liquid cooling systems have been commercialized, but they work with low efficiency. MCPs are like heat exchangers, which consist of many channels through which coolant flows that absorb heat from the batteries in contact with the cold plate.

Mini-channels are used in cold plates because they offer less thermal resistance and more heat transfer area per unit-volume. Channel geometries of cold plates could be circular, square, rectangular or polygonal with hydraulic diameters in the range of 1 to 6mm. They offer high heat transfer rates and can be easily installed with prismatic batteries<sup>18</sup>. A parametric study on a serpentine mini-channel cold plate by varying parameters like channel width and position was carried out<sup>19</sup>. By varying number of mini-channels, direction of flow and inlet temperature. It is noted that the mass flow rate of the coolant effectively decreases the maximum temperature of the battery, but after an optimum mass flow rate, the reduction in the maximum temperature of the battery is minimal<sup>20</sup>.

In a study width of the mini-channels and the number of channels varied and the results showed that with an increase in the number of mini-channels, the maximum temperature of the battery decreases, and temperature uniformity is also increases, but after an increase in the number of mini-channels by more than five, there is not much change in the peak temperature of the battery<sup>21</sup>. The effect of turbulent flow in the mini-channels both numerically and experimentally studied. It was observed that with an increase in discharge rates, battery temperature is increasing. It was also observed that the thermocouples which are near to the electrodes are showing high temperatures than those which are located at the center of the battery surface<sup>22</sup>.

The effects of layout of the mini-channel, number of mini-channels, and coolant inlet temperature. The authors observed that channels in the length direction yielded better results than the channels in the width direction. They have

also inferred that the coolant inlet temperature has a small influence on pressure drop and maximum temperature difference. The influence of cooling channel number and inlet temperature of the coolant, considering serpentine channel layout is numerically investigated. In addition effect of flowing direction of channels in width and length layout direction and noted that

Length wise is superior and also the effect of inlet temperature of the coolant has little influence on temperature and pressure drop. The peak temperature of cooling system rises with the increase of inlet temperature of the coolant<sup>23</sup>. Investigations with different coolants like water, engine oil, ethylene glycol and their corresponding nano-fluids concluded that adding nanofluids to fluids having lower thermal conductivity is more effective than adding nanofluids to fluids having high thermal conductivities<sup>24</sup>.

A serpentine flow design for coolant flow with MCP was designed with two inlets and two outlets. They studied the effects of flow rates, flow directions, and the width of the channel. They observed that the flow directions and location of the coolant inlet and outlet effectively change the battery's maximum temperature and power consumption<sup>25</sup>.

A battery pack consisting of 4 batteries and 5 cold plates and varied the number of MCPs and cooling direction. The results show that more amount of heat will be accumulated in the middle of the battery pack. It is inferred that more MCPs should be arranged closer to the middle of the battery pack and also observed that the cooling direction of channels in the cold plate can also decrease the temperature difference of the battery pack<sup>26</sup>. A numerical work is done with four batteries and five cold plates and studied the effects of mass flowrate of coolant, no. of cold plates, channel distribution and cooling direction. The study revealed that cold plates should be arranged as close as possible to the middle of the battery as the heat accumulates easily in the battery pack and more cooling channels are placed. Moreover, the uniformity of temperature distribution of the battery pack depends on the directions of the channels in the cold plate<sup>26</sup>.

A streamlined shape for cold plate channels is introduced, and the results show that because of the streamlined shape, resistance to flow was reduced, resulting in a reduction thereby increasing the heat exchanger efficiency. It is noted that because of the streamlined shape, the temperature uniformity of the cold plate also increased<sup>27</sup>. Bio-inspired tree-type and leaf-type mini-channels were employed and compared with regular rectangular-type channels. It is inferred that the thermal performance was better with bio-inspired patterns<sup>28</sup>.

A study with different profiles of MCPs for the battery thermal management application is proposed and investigates the role of the profile of the mini-channel on the performance of the battery thermal management application. The results show that the profile of the mini-channel influences the performance of MCP<sup>29</sup>. The effect of vibration on heat transfer is studied referring to MCPs as a part of BTMS. The results indicated that vibration had the effect of enhancing the

heat transfer capacity of the cold plate, which was related to the frequency, amplitude and mass flow rate. The authors in addition observed the effect of fillets to the cross section and noted that fillets enhanced the heat transfer<sup>30</sup>.

It is observed from the literature that although there were many studies reported on the mini-channel- enabled cold plates for battery thermal management, it is noted that very complicated patterns for mini- channels were used. It is further noted that there is limited research on BTMS using mini-channel cold plates compared to other BTMSs. Moreover, a few works have focused on simple straight rectangular mini-channels. There is not much information available in the literature on how cross-sections of mini-channels will influence the cooling performance of a battery pack. Considering the need for a simple design of BTMS with a liquid cooling system, a systematic numerical study is carried out using ANSYS platform. The study aimed at recommending a simple design between two designs considered with the use of MCP for BTMS work on a prismatic battery pack.

In the present work, systemic and extensive simulations on two simple designs are performed, and the effect geometry-related parameters and flow rates are employed on mini-channel cold plates with rectangular, zig-zag and wavy channels<sup>31</sup>. The computational work was carried out using ANSYS- Fluent R1 version software, systematically applying it to a single cell, module, and battery pack. The effect on the battery peak temperatures with active cooling through mini-channel cold plates under different discharge rates and other geometrical and flow parameters pertained to MCP has been observed. The two cases have been compared for their efficacy

in lowering the peak battery temperature and maintaining uniform temperature across cells in a battery pack considering varying conditions.

**II. NUMERICAL METHODOLOGY**

In an attempt to employ a liquid cooling strategy for effective thermal management, a mini-channel cold plate has been used, starting with a single cell to a battery pack, and the modelling works have been carried out in the following sequence.

- A single LIB cell and a mini-channel cold plate
- Effect of cross-section of channels of a mini-channel cold plate
- LIB pack and mini-channel cold plates [Each cell is inserted by two adjacent MCPs. Design-1]
- Design-1 with wavy channels
- LIB pack and mini-channel cold plates [Every five cells are inserted between two MCPs.Design-2]
- Design-2 with zig-zag channels

**III. SIMULATION STUDIES**

*A. Simulation Studies on a Single LIB Cell and a Mini-Channel Cold Plate*

Before embarking on modelling a battery pack with a mini-channel cold plate, a single LIB cell is simulated to study the heat generation in a battery. The specifications of a prismatic LIB cell and the properties of cell layers are given Table.1

Table 1 Specifications of Prismatic LIB Cell and Properties of LIB Cell Layers

Parameter		Value		
Nominal capacity		14.6 Ah		
Minimum potential		3.0 V		
Maximum potential		4.2 V		
Cathode		LiMn <sub>2</sub> O <sub>4</sub>		
Anode		Graphite		
Electrolyte		Polymer based		
Dimensions		192 mm × 145 mm × 5.4 mm		
Layer	ρ, kg/m <sup>3</sup>	C <sub>p</sub> ,(J/kg.K)	k (W/m.K)	L <sub>i</sub> (mm)
Positive electrode	1500	700	5	150
Negative electrode	2500	700	5	145
Separator	1200	700	1	12
Positive current collector	2700	900	238	20
Negative current collector	8960	385	398	10

Generally, prismatic LIBs are developed by accumulating several sandwich layers, like anode- separator-cathode. It is difficult to mention the details of each and every single layer in the software ANSYS FLUENT. Therefore, a simplified method is adopted by considering the battery as it is made up of homogeneous materials, and the effective properties in the software are used. For example, the density is calculated as given by Eq. [1].

$$\rho = \frac{\sum L_i \rho_i}{\sum L_i} \tag{1}$$

Also, the other effective properties such as specific heat and thermal conductivity for the battery material were also calculated. For modelling purpose, ANSYS FLUENT software 2023 R1 has been used. The Newman, Tiedemann, Gu, and Kim (NTGK) model, a widely accepted model for electrochemical modelling of a battery cell, was adopted based on input parameters to study the variation of peak temperature in the LIB. Nominal capacity of lithium-ion

battery is 14.6 Ah. Reference capacity is also given same as nominal capacity. Battery's depth of discharge is given as zero percentage. After enabling the battery model with required properties including user defined functions for both active material and tabs given in ANSYS FLUENT are used.

➤ *Governing Equations for the Lithium-Ion Battery Cell*

The heat generation in the battery pack has been studied by using a simple semi-empirical electro- thermal NTGK model and applied in the software. The polarization expressions and temperature of a single lithium-ion battery are given by Equations:

$$\frac{\partial \rho C_p}{\partial t} = \frac{\partial}{\partial x} \left( \sigma_+ \frac{\partial \phi_+}{\partial x} \right) + \frac{\partial}{\partial y} \left( \sigma_+ \frac{\partial \phi_+}{\partial y} \right) + \frac{\partial}{\partial z} \left( \sigma_+ \frac{\partial \phi_+}{\partial z} \right) + Q_g \quad (2)$$

$$\nabla(\sigma_+ \nabla \phi_+) = -(J_{ECh} - J_{short}) \quad (3)$$

$$\nabla(\sigma_- \nabla \phi_-) = (J_{ECh} - J_{short}) \quad (4)$$

$$J_{ECh} = \alpha Y [U - (\phi_+ - \phi_-)] \quad (5)$$

Where,

$\phi_+$  = Phase potentials of positive electrode

$\phi_-$  = Phase potential of negative electrode

$\sigma_+$  = Electrical conductivity of positive electrode

$\sigma_-$  = Electrical conductivity of negative electrode

$Q_g$  = Heat generated in the battery

$J_{short}$  = Current transfer rate

$J_{ECh}$  = Volumetric current transfer rate.

$Y$  = Conductance of the battery which depends on DoD

$U$  = Open circuit voltage of the battery which depends on DoD.  $U$  and  $Y$  can be expressed as follows

$$U = a_0 + a_1(DoD) + a_2(DoD)^2 + a_3(DoD)^3 \quad (6)$$

$$Y = a_4 + a_5(DoD) + a_6(DoD)^2 \quad (7)$$

Where  $a_0$  to  $a_6$  are the fitting parameters which depends on the reference capacity and can be obtained through experimental results. Therefore, the fitting parameters have been incorporated as given in the literature and have been used to calculate  $U$  and  $Y$ , the depth of discharge (DoD) can be given by:

$$DoD = \frac{J_0 t}{QT} \quad (8)$$

Where,

$J$  = Current density distribution,  $t$  = Flow time during the discharge protocol,

$QT$  = Capacity of the electrodes in (Ahm<sup>-2</sup>)

➤ *Boundary conditions for the LIB cell*

$$t = 0, T(x, y, z) = T_0 \quad (9)$$

Where,  $T_0$  is the initial temperature of both active material (battery) and tabs considered as 300 K. The atmospheric temperature is also set as same as initial temperature. All the walls of the active material and tabs are given free convection boundary condition with convection heat transfer coefficient of 5 W/m<sup>2</sup>K. In addition, the walls between the cell and the tabs are set as thermal coupled interfaces.

The simulations are carried out by solving the above-mentioned governing equations, the properties of cell layers and using the given boundary conditions. Initially a grid independence has been done at 5C discharge rate, to determine the size of mesh to be used for further simulations, as shown in Figure 1[b]. Meshes with different number of elements ranging from 54,000 to 2,00,000 elements has been used to simulate the battery's peak temperature. The maximum temperature of the cell for different meshes with different number of elements are compared for grid independence study. It is observed that when the number of elements are more than 1,06,000 the cell's maximum temperature almost remained constant. Therefore, the mesh size with 1,06,000 elements has been chosen for the study. The chosen prismatic LIB cell, computational mesh and grid independence results are in Figure 1.

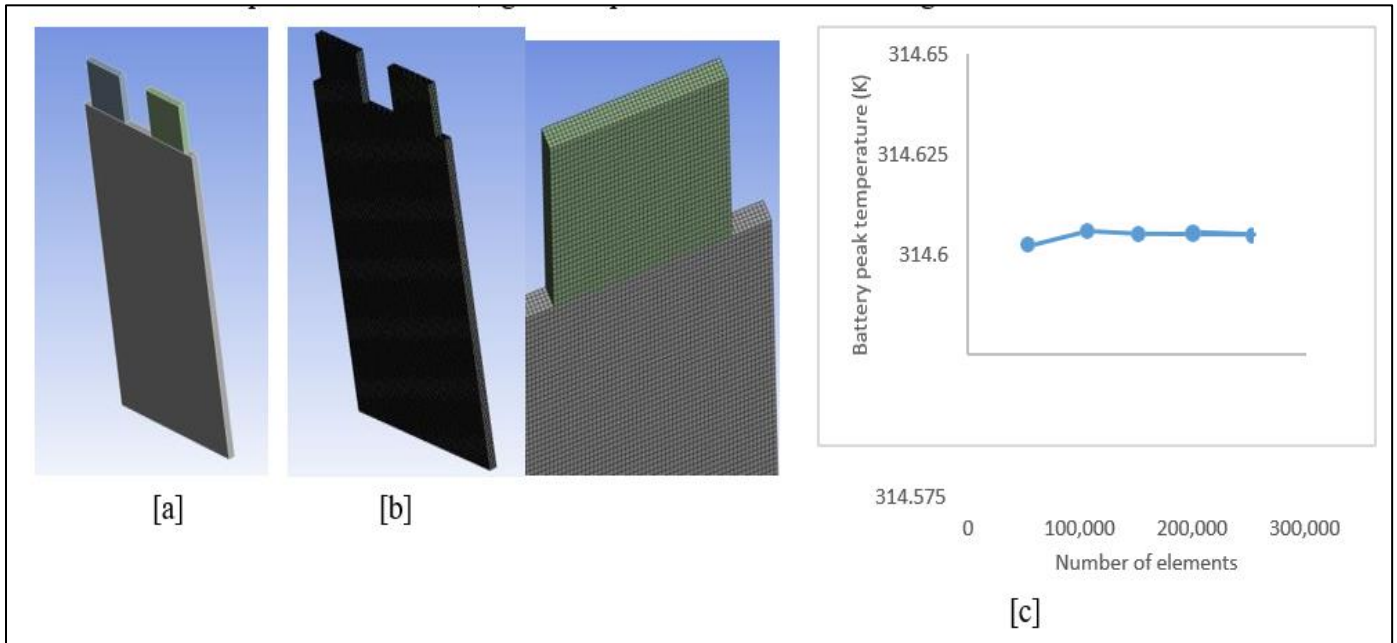


Fig 1 Illustration of [A] Prismatic LIB Cell [B] Computational Mesh of LIB Cell and [C] Grid Independence Study of LIB Cell.

*B. Simulation studies on a mini-channel cold plate*

➤ *Governing Equations For The Mini-Channel Cold Plate*

The conservation of energy equation for water in the mini-channels is given by

$$\rho_c C_{p,c} \frac{\partial T_c}{\partial t} + \nabla \cdot (\rho_c C_{p,c} \vec{v} T_c) = \nabla \cdot (k_c \nabla T_c) \tag{10}$$

Where,  $\rho_c$ ,  $C_{p,c}$ ,  $k_c$  and  $T_c$  are the density of water, specific heat capacity of water, thermal conductivity of water and temperature of the water and  $\vec{v}$  is the velocity vector of water. Conservation of mass equation for water in the mini-channels is given as

$$\nabla \cdot \vec{v} = 0 \tag{11}$$

Conservation of mass equation for the water in the mini-channels is given as

$$\rho_c \left[ \frac{\partial \vec{v}}{\partial t} + (\vec{v} \cdot \nabla) \vec{v} \right] = -\nabla P + \mu \nabla^2 \vec{v} \tag{12}$$

Where  $P$  and  $\mu$  are the static pressure and dynamic viscosity of the water.

➤ *Boundary Conditions for the Mini-Channel Cold Plate*

Channels inlet is given as mass flow of  $5e-4$  kg/s, channels outlet is given as pressure outlet with zero-gauge pressure. Heat flux of  $5250 \text{ W/m}^2$  is given to the both sides of the cold plate wall and the walls of the cold plate are given convection heat transfer coefficient of  $5 \text{ W/m}^2\text{K}$ . Inlet temperature of 298 K is given to the coolant. For the fluid-cold plate interface, no slip boundary condition has been given. The heat flux value is taken from the data given by Liu et al. 2018 during 3C discharge rate when the cold plate is surrounded by five batteries on each side.

On the similar lines, a computational mesh is created for MCP and a grid independence study is done as detailed in Figure 2. Simulations are done by solving the governing equations using the given boundary conditions [Sec:3.2.1]. A grid independence has been done to determine the size of the mesh to be used for the simulations, as shown in Figure 2. Meshes with different numbers of elements ranging from 4,60,00 elements to 10,61,000 elements have been used to simulate the maximum temperature of a cold plate. The maximum temperature of the cold plate and pressure drop for different meshes with different number of elements are compared for grid independence study. It is observed that when the number of elements is more than 7,70,000, the maximum temperature of the cold plate and pressure almost remain constant. Therefore, the mesh size with 7,70,000 elements has been chosen for the study.

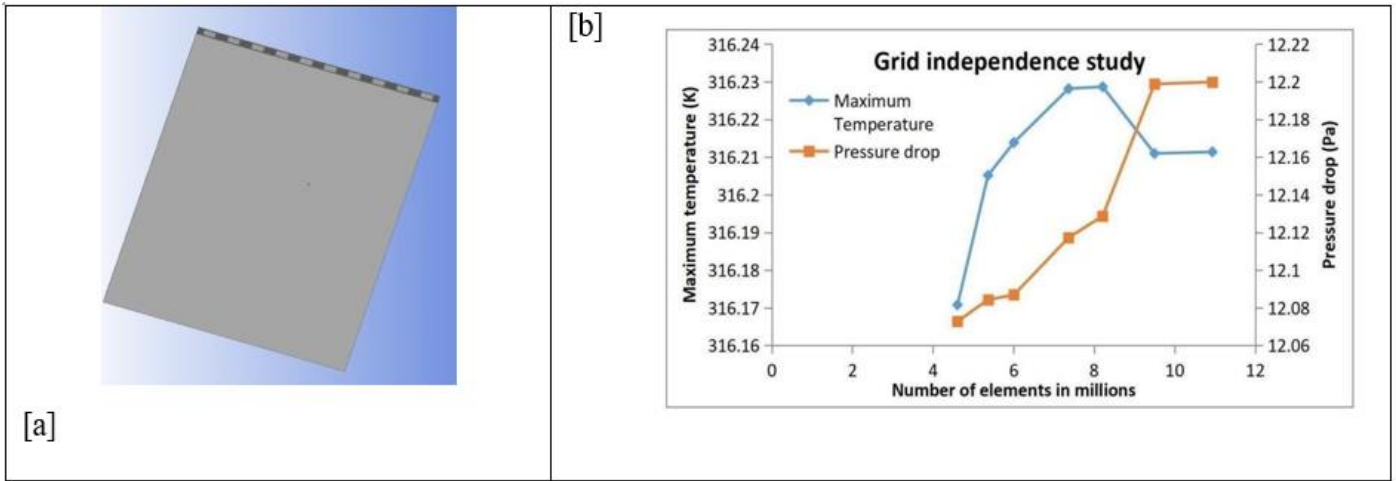


Fig 2 [A] Mini-Channel Cold Plate and [B] Grid Independence Study of MCP

A mini-channel cold plate with dimensions 180 mm × 100 mm × 4mm and channels 5mm× 3mm has been modeled as shown in Figure 3.5. The gap between two channels is 5mm. Aluminum is used as the cold plate material, and water

is considered the coolant. The properties of aluminum and water are given in Table 2.

Table 2 Properties of Aluminum and Water

Material	$\rho(kg. m^{-3})$	$C_p (J. kg. K^{-1})$	$k (W. m^{-1}. K^{-1})$	$\mu(kg. m^{-1}. s^{-1})$
Aluminum	2719	871	202.4	-
water	998.2	4182	0.6	0.000184

In addition, to check the efficacy of present work modelling data, validation with numerical and experimental data for both LIB cell and MCP available in the literature is carried out and presented as Figure 3<sup>32</sup>.

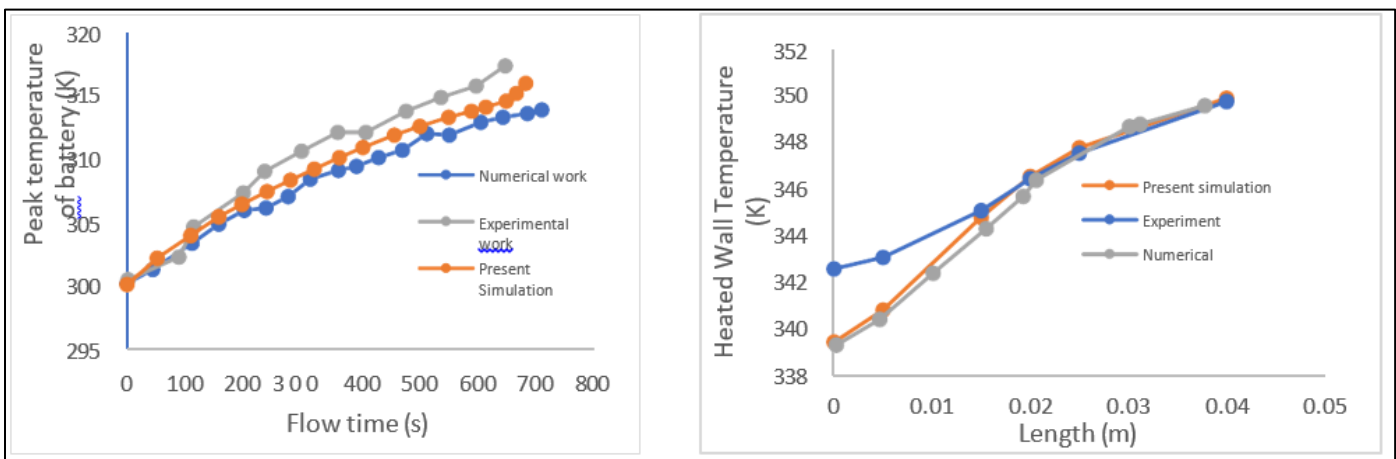


Fig 3 Validation Results of LIB Battery Cell At 5C and Mini-Channel Cold Plate

*C. Mini-channel cold plate for the effective thermal management of lithium ion-cell*

As mentioned in the above sections, the use MCP has been used for BTMS requirements and hence the simulation of a cell along a MCP are done as shown in Figure 4. Mini-channel Cold Plates, when attached to battery cells to cool the battery, a large quantity of heat from the batteries will be carried by the coolant flowing through the mini-channels. For the present study, the mini channel cold plate is taken with the

same length and width as that of the cell is taken with a thickness of 4 mm. A maximum of ten channels are chosen, each with dimensions of 3mm × 8mm so as to suit to the cooling requirement of a chosen cell. The governing equations for lithium ion-cell, mini-channel cold plate and boundary conditions for lithium ion-cell, mini-channel cold plate are applied here except that the initial temperature of cold plate which is taken same as battery that is 300K.

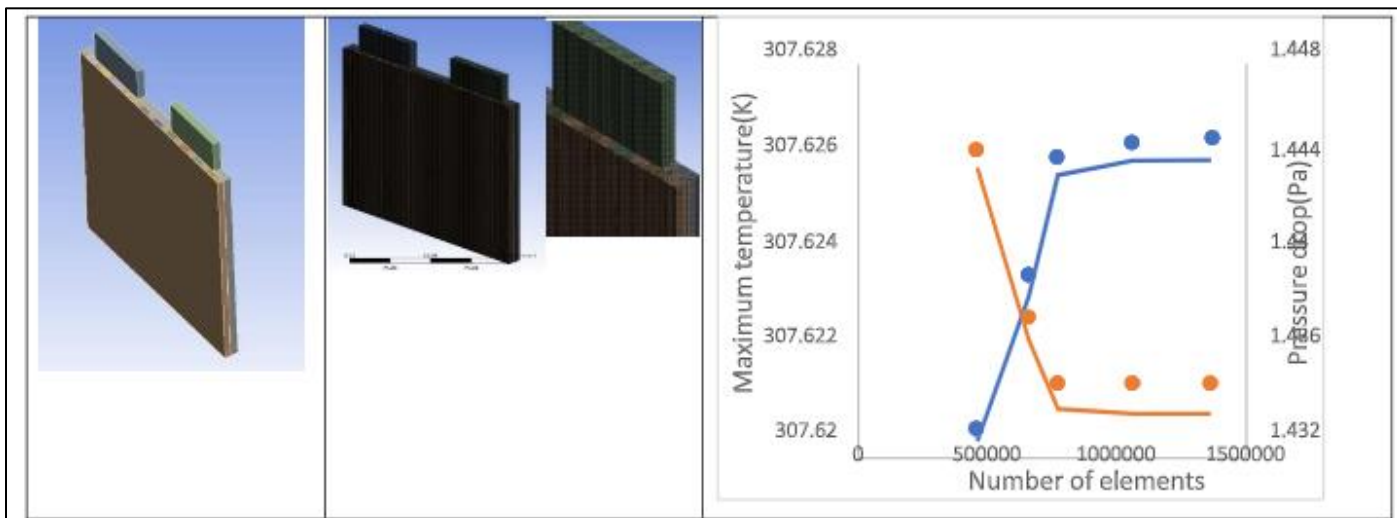


Fig 4 Illustration of [A] Prismatic LIB Cell with MCP [B] Computational Mesh of LIB Cell and MCP [C] Grid Independence Study of LIB Cell with MCP.

The variation of MCP temperature with mass flow rate and the corresponding pressure drop values are obtained as shown in Figure 5, for use in subsequent simulations.

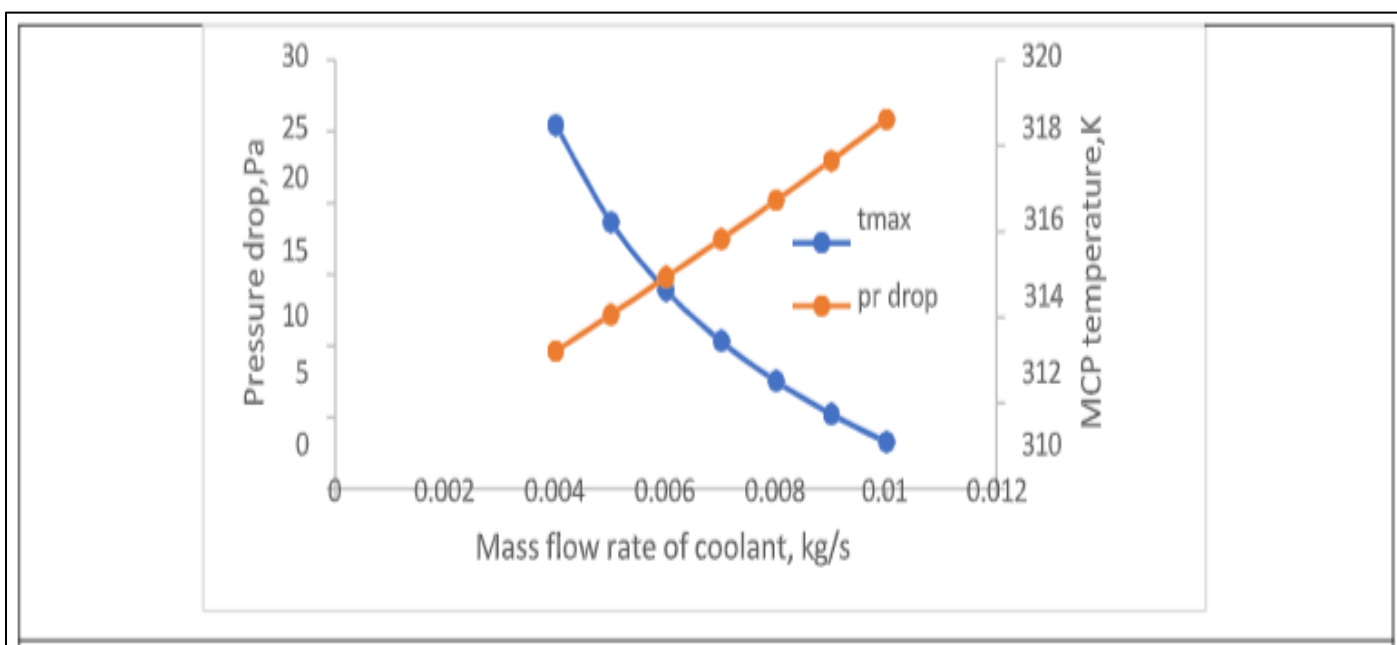


Fig 5 Variation of MCP Temperature and Pressure with Inlet Mass Flow Rate of Coolant

**D. Simulation studies on LIB pack and mini-channel cold plates [Design-1]**

After understanding the behavior of a cell, MCP, combination of cell and MCP, through simulations, further work is taken up for modelling a battery pack along with MCP considering

each cell is inserted by two adjacent MCPs and denoted as Design 1. Figure 6 shows the details of Design-1 along with computational mesh and grid independence details.

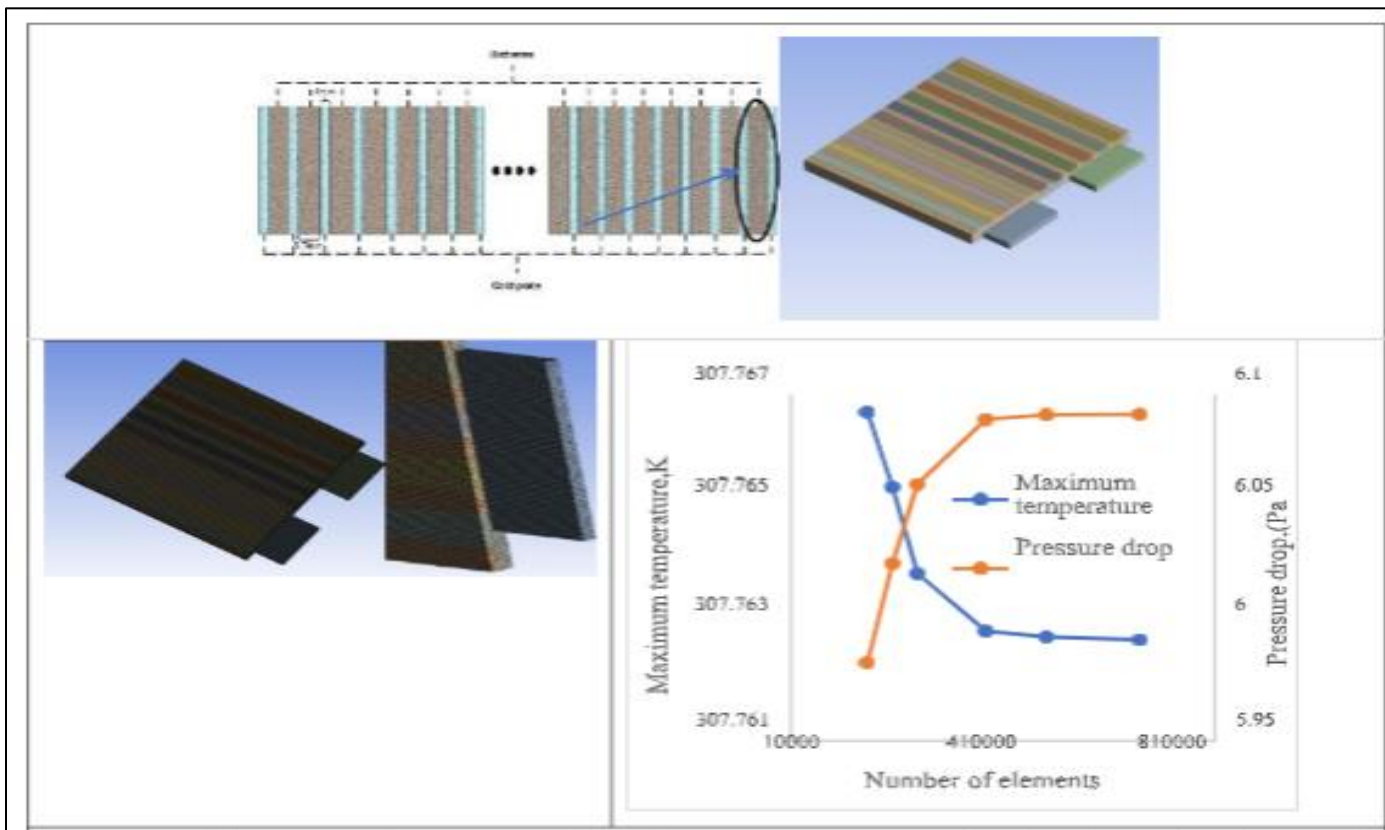


Fig 6 Illustration of [A] Battery Pack-Design 1 [B] Computational Mesh of LIB Cell and [C] Grid Independence Study for Part of Design-1.

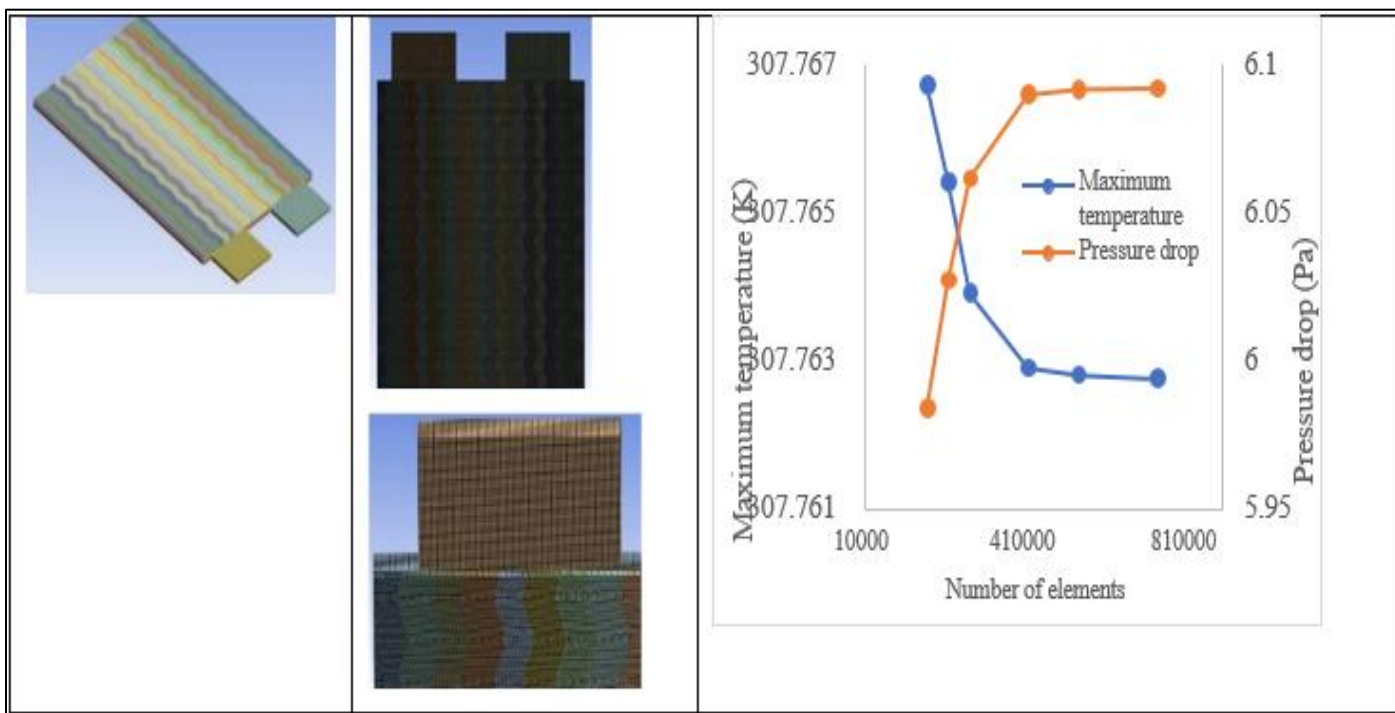


Fig 7 Illustration of [A] Prismatic Lib Cell with Wavy Channel [B] Computational Mesh of Lib Cell With Wavy Channel Mcp [C] Grid Independence Study Of Lib Cell And Way Channel Mcp.

*E. Simulation studies on LIB pack and mini-channel cold plates [Design-2]*

Simulation studies on another design is taken up for modelling a battery pack along with MCP considering every

five cells are inserted between two MCPs and denoted as Design 2. Figure 8 shows the details of Design-2 along with computational mesh and grid independence details.

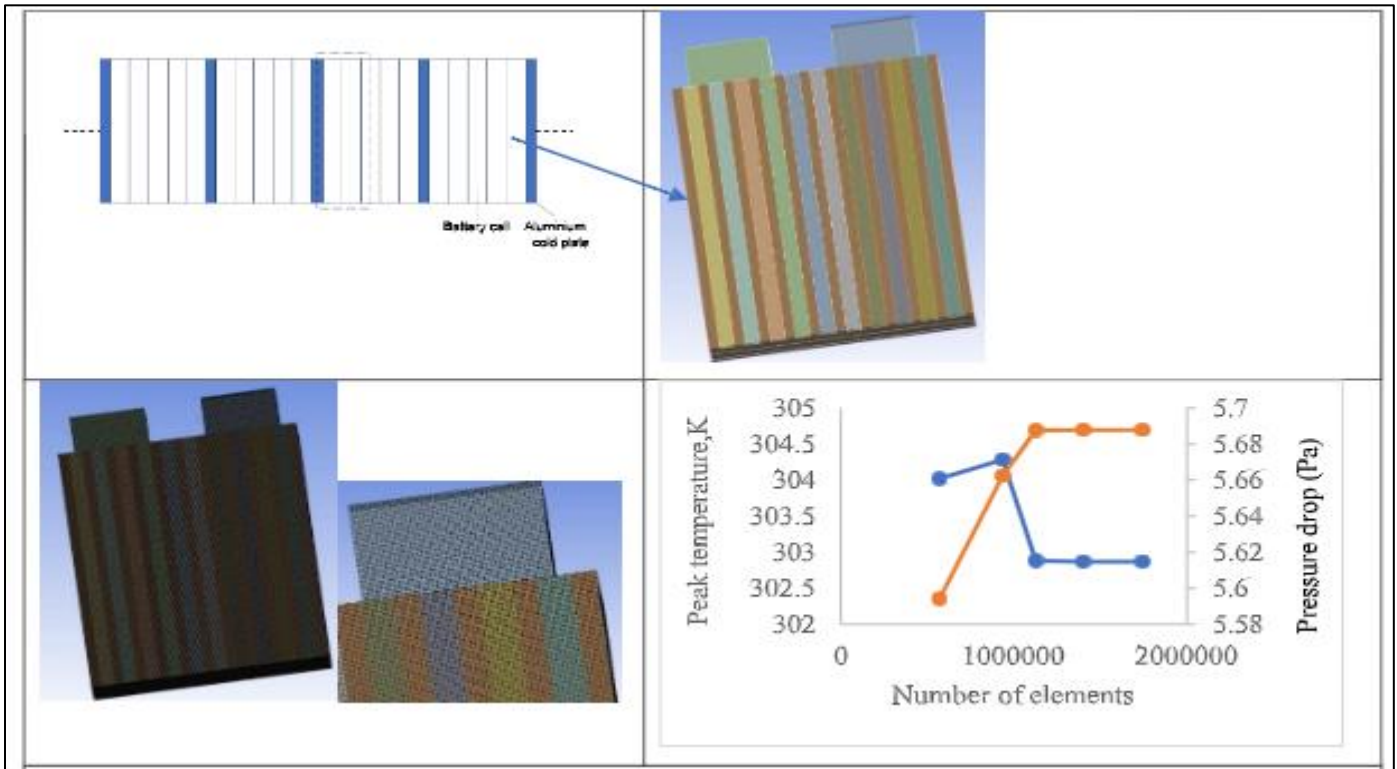


Fig 8 Illustration of [A] Battery Pack-Design 2 [B] Computational Mesh of LIB Cell And [C] Grid Independence Study for Part of Design-2.

**IV. RESULTS AND DISCUSSION**

After doing a grid independence study and validating the results as explained in numerical methodology, simulations have been done to obtain peak battery temperature and peak temperature difference for different cases, and the results obtained are discussed appropriately. The cases studied are listed below:

- A. A single LIB cell without cooling under three different discharge rates.
- B. A single LIB cell and a mini-channel cold plate
- C. Effect of cross-section of channels of a mini-channel cold plate

- D. LIB pack and mini-channel cold plates [Each cell is inserted by two adjacent MCPs. Design-1]
- E. Design-1 with wavy channels
- F. LIB pack and mini-channel cold plates [Every five cells are inserted between two MCPs.Design-2]
- G. Design-2 with zig-zag channels

*A. A Single LIB Cell without Cooling Under Three Different Discharge Rates.*

As an initial step, a single lithium-ion battery cell has been simulated by adopting the governing equations and boundary conditions for 3 different discharge rates: 1C,3C, and 5C. Figure 9 depicts the variation of the peak temperature of the LIB cell with flow time at different discharge rates.

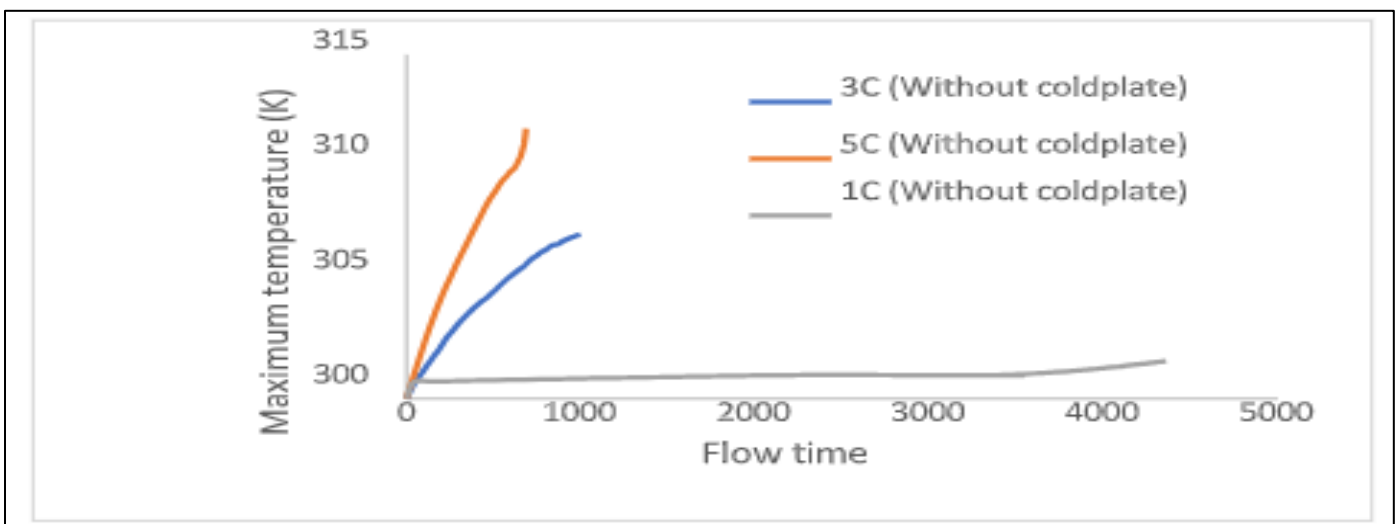


Fig 9 Variation Of Peak Temperature During Discharge Rates Of 1C, 3C, And 5C.

The adopted simulation software well predicted the temperature-time histories of LIB for different discharges. It is observed that with increase in discharge rate, the discharge time got reduced but with increase in temperature. This indicates that the higher the discharge rate at a given ambient temperature, the greater the requirement for thermal management. Figure 10 shows the battery temperature

contours at discharge rates of 3C and 5C respectively. From the contours, it can be observed that the temperature of lithium-ion cells is not uniform, and this non-uniformity is more at higher discharge rates like 5C. Therefore, it is very much required to maintain the peak temperature difference less than 5°C.

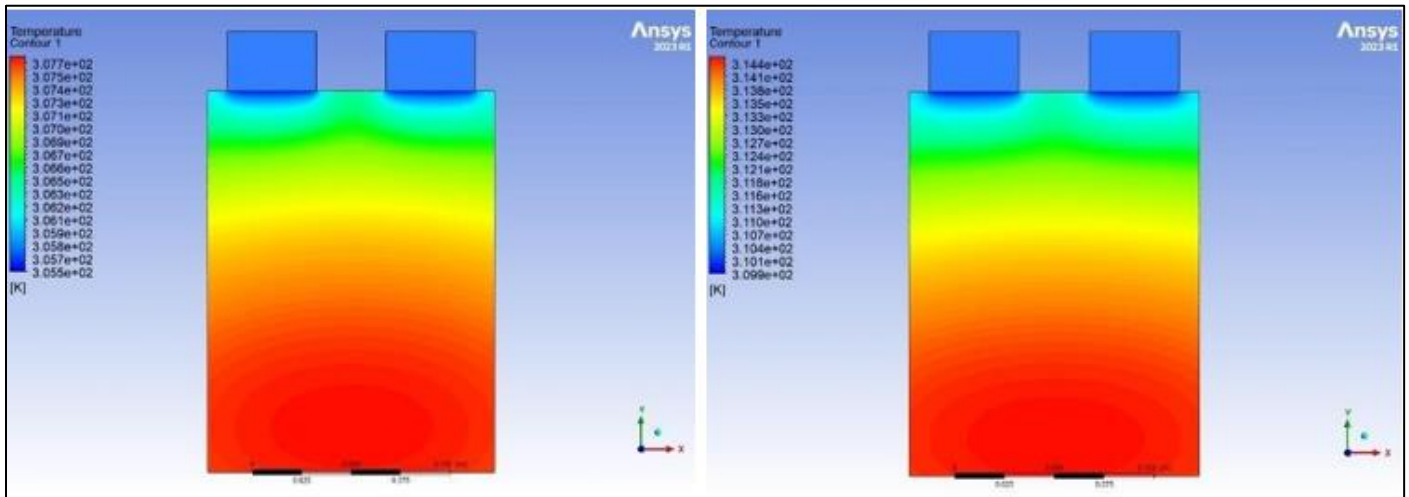


Fig 10 Temperature Contours of Battery for 3C and 5C Discharges

**B. Studies on Influencing Factors of MCP for Effective Thermal Management**

For effective thermal management, the MCP should be effective and provide the lowest possible peak temperature, and the lowest temperature difference. First the MCP is simulated during the inlet mass flow rate is 5 kg/s, wall heat flux is 5250 W/m<sup>2</sup> with ten channels and the width of the mini channel as 5mm. The maximum temperature of 316.2207 K with the temperature difference of 13.1943 K is obtained with a pressure drop of 12.1726 Pa. Temperature contour of the wall exposed to heat flux is

Shown in Figure 4.4.

➤ *Effect of Width of Mini-Channels*

The MCP should have a number of channels in order to accommodate as much coolant as possible. To observe the effectiveness of cooling with the number of channels, it is observed that as the width of the channel increases, the maximum temperature of the mini-channel cold plate decreases, as shown in Figure 11[a]. It is also observed that pressure drop decreases with the width of the mini-channel, as shown in Figure 11[b].

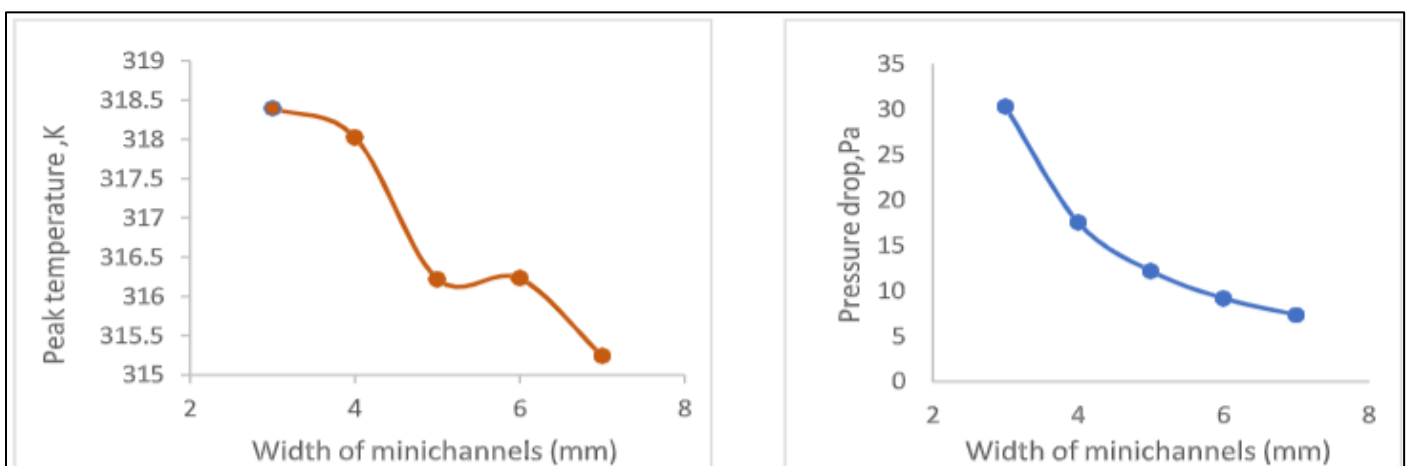


Fig 11[A] Variation of Peak Temperature of Cold Plate with Width of Mini-Channels. Fig 11[B]: Variation of Pressure Drop with Width of Mini-Channel

➤ *Effect of Mass Flow Rate*

In addition to a number of channels, the dissipation of heat depends on the inlet mass flow rate of the coolant. Thus, the simulations that have been carried out for different flow

rates. It is noted that as the inlet flow rates are increased, the peak temperature of the cold plate has decreased. It is also observed that the pressure drop increases with mass flow and found to be detrimental as it increases the power

consumption. Therefore, an optimum mass flow needs to be found for a given configuration, and it is observed that after increasing the mass flow rate more than 0.006 kg/s, there is not much decrease in the maximum temperature of the cold plate, but the pressure drop is increasing. Therefore, for the present study, an inlet mass flow rate of 0.006 kg/sec has been

found to be optimum.

Figures 12[a] and [b] illustrates the variation of peak temperature and pressure drop with mass flow rate.

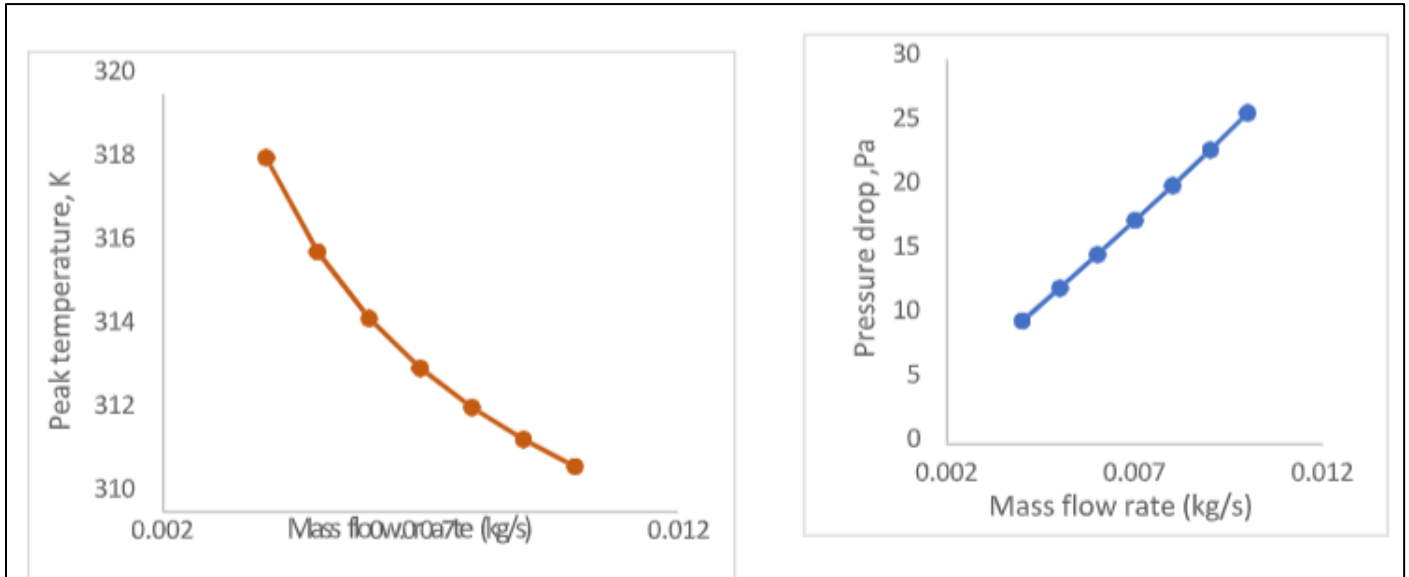


Fig 12[A]: Variation of Peak Temperature of Cold Plate with A Mass Flow Rate Fig 12[B]: Variation of Pressure Drop with Mass Flow Rate

➤ *Effect of number of mini-channels*

Further simulations are focused on observing the effect of the number of channels increasing and the peak temperature of the cold plate decreasing, as shown in Figure 13[a]. It is observed that the pressure drop is also decreasing, as shown in Figure 13[b]. It is also observed that after increasing the number of channels to more than seven, there is not much decrease in the pressure drop.

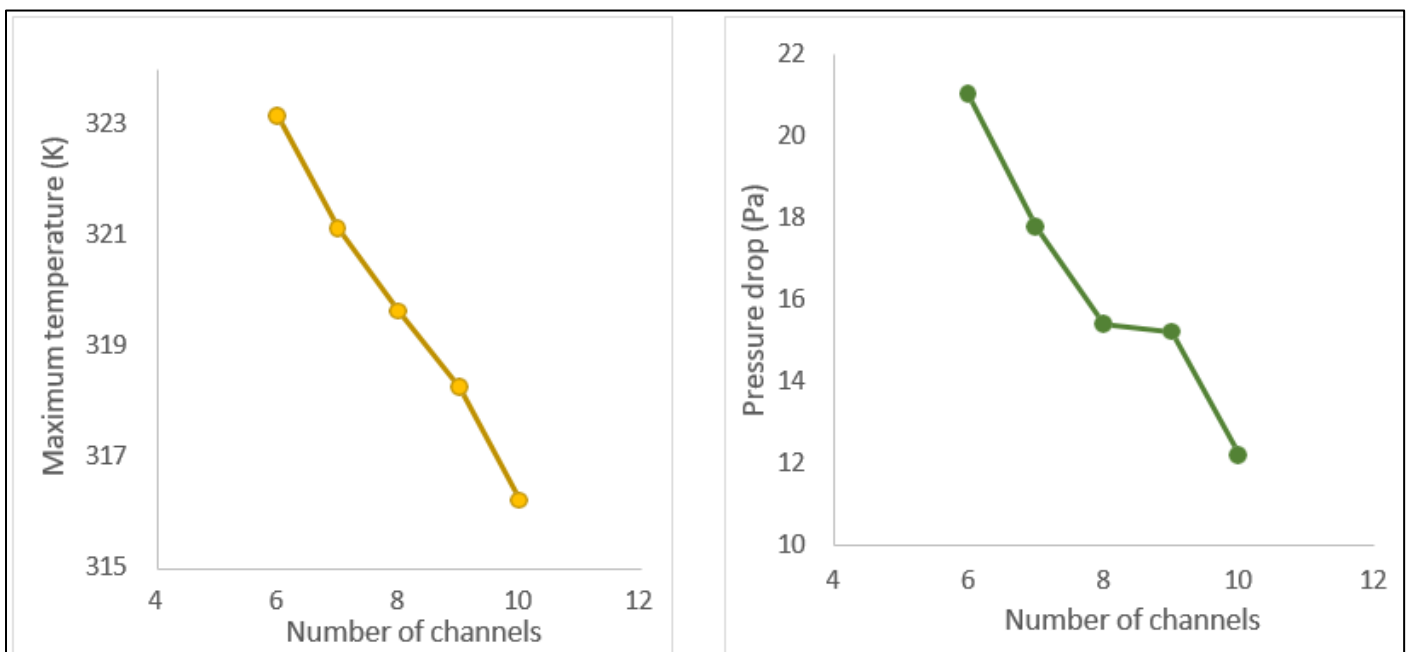


Fig 13[A]: Effect of Number of Channels on Maximum Temperature of Cold Plate [B]: Effect of Number of Channels on Pressure Drop.

➤ *Effect of Cross Section of Mini-Channels*

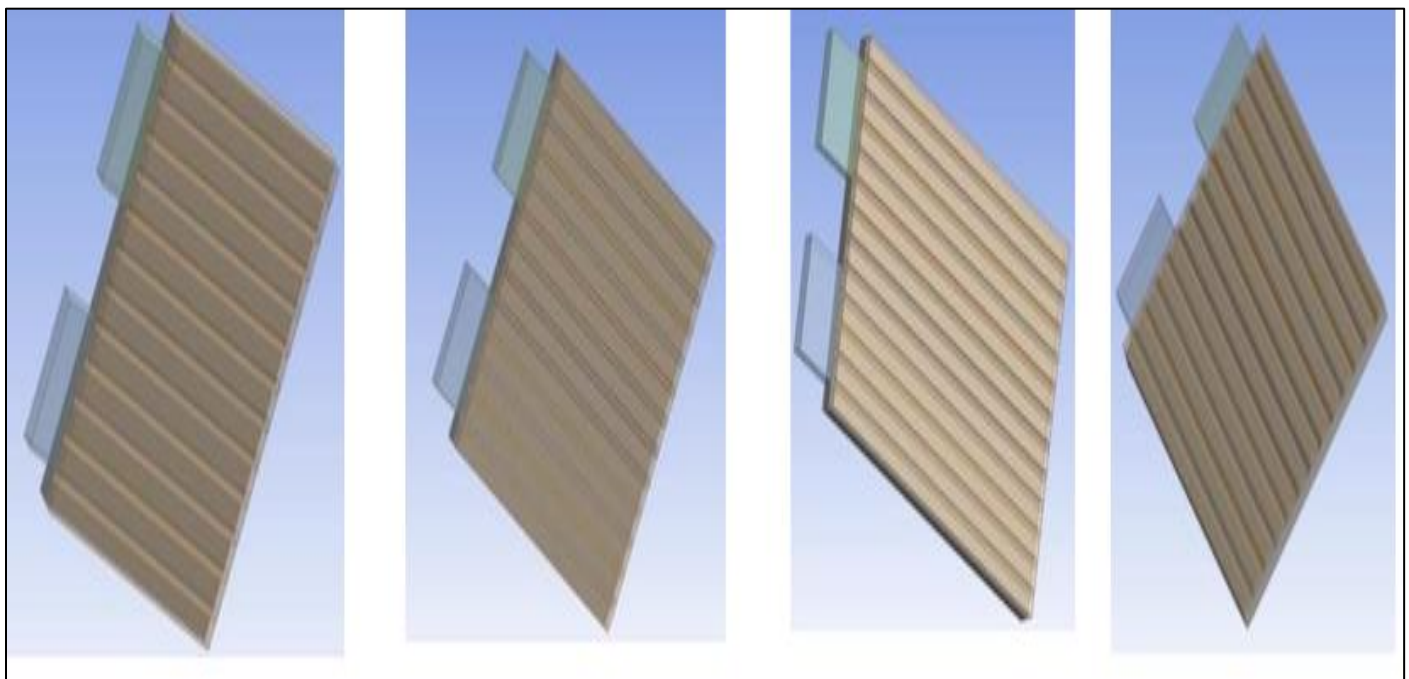


Fig 14 Battery with Cold Plate of Circular, Rectangular, Hexagonal and Rhombus Cross Sections Respectively

To know the effect of a cross-section of mini-channels for the cooling of batteries, a cross-section of channels varied from circular, rectangular, hexagonal to rhombus, respectively, as shown in Figure 14. The cross-sectional area of the four cross-sections has been kept constant, and the mass flow rate has to  $5 \times 10^{-3}$  kg/s,  $5 \times 10^{-4}$  kg/s,  $5 \times 10^{-5}$  kg/s, and  $5 \times 10^{-6}$  kg/s, respectively. It was observed that by increasing the mass flow rate, the batteries' peak temperature decreases for all the cross sections, but at a particular mass flow rate, there is no

significant change in the peak temperature, as shown in Figure 15. The reason is since the channels are straight, the heat transfer surface area of different channels does not change much

But compared to all other cross sections rhombus cross section is providing lower temperatures. Thus the rhombus cross section can be used at higher discharge rates particularly when the heat generation values are high.

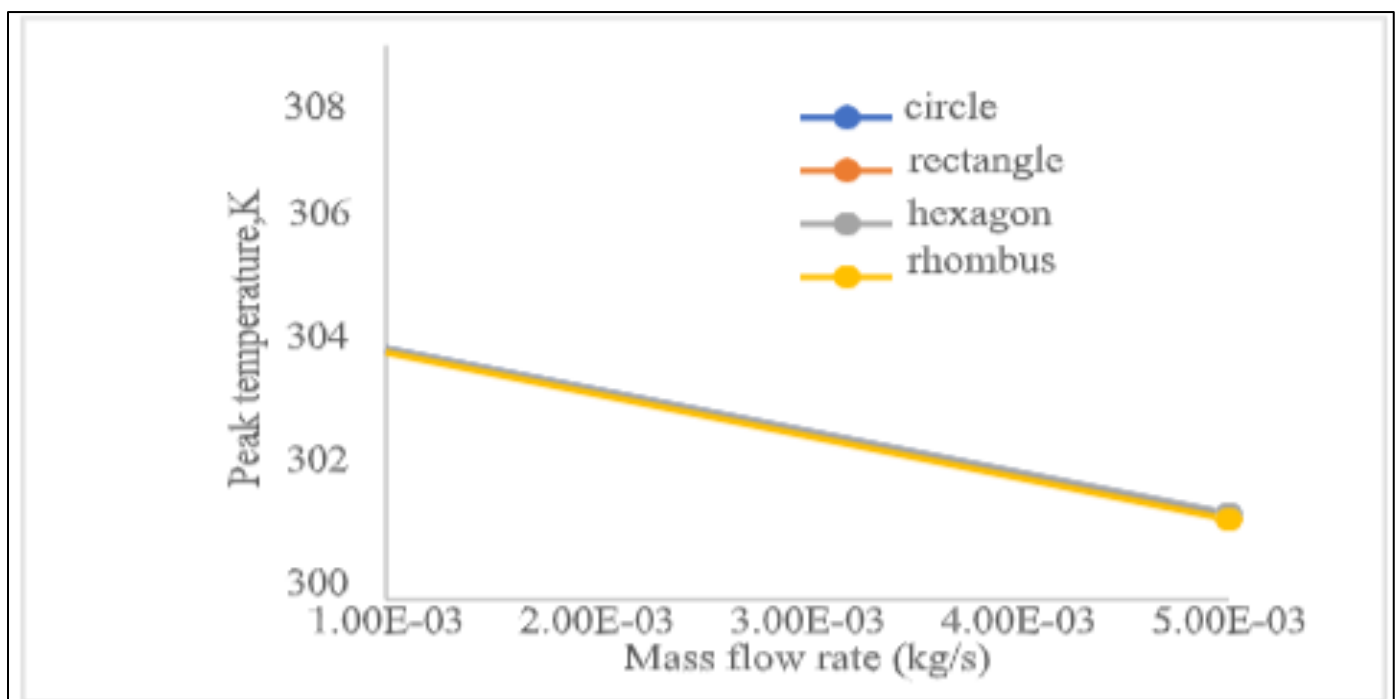


Fig 15 Variation of Peak Temperature of MCP With Respect To Mass Flow Rate for Different Cross Sections.

**C. Simulation Results of a Single LIB Cell With an MCP**

Therefore, it is observed that the mini-channel cold plate is effectively cooling the lithium-ion cell. Figures 16[a] and 16[b] show the temperature contours of lithium-ion cells with mini-channel cold plates under discharge rates of 3C and 5C, respectively, during mass flow rate of 5e-4 kg/s. From the contours, it is observed that the mini-channel cold plate is effectively reducing the temperature difference of the lithium-ion cell less than 5°C, thereby increasing the temperature uniformity. Therefore, it is observed that good thermal management obtained with MCP for the LIB cell.

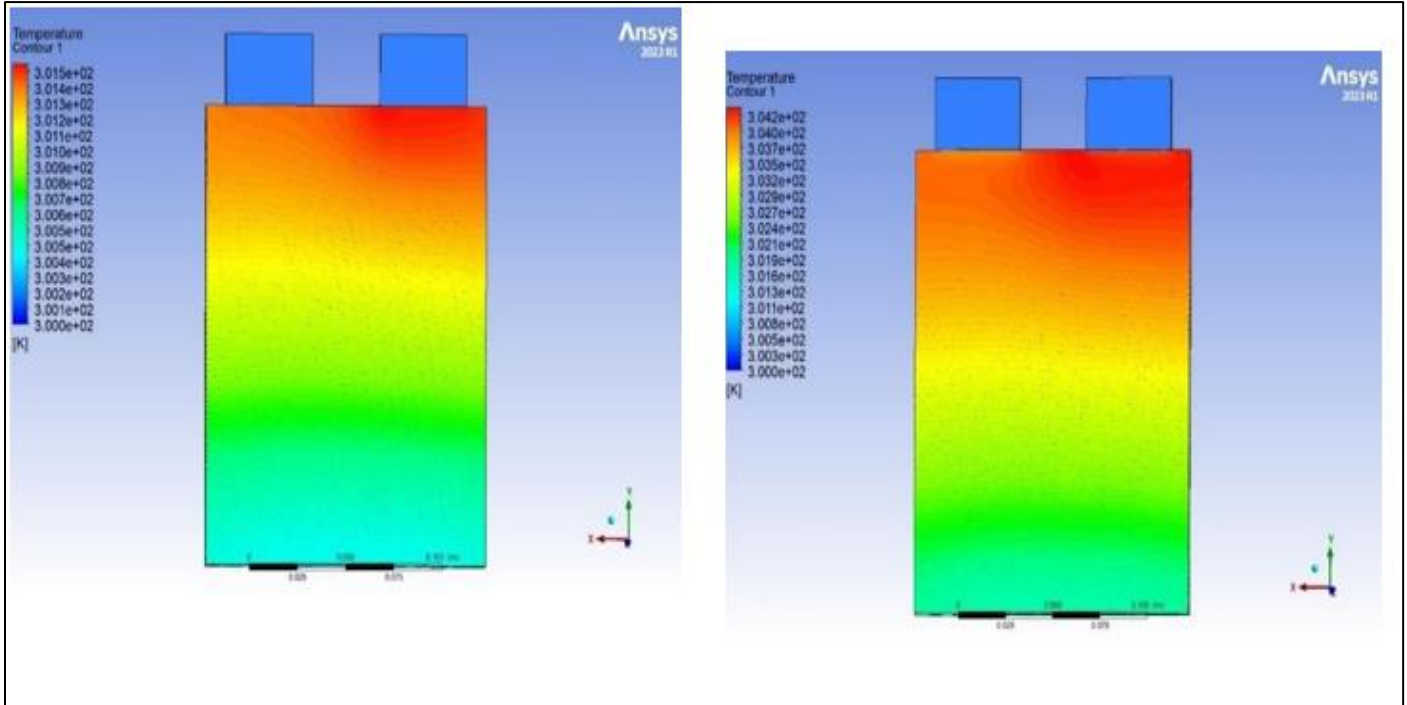


Fig 16[A]: Temperature Contours Of Lib with MCP Under 3c. Figure 16[B]: Temperature Contours of Lib with MCP Under 5c.

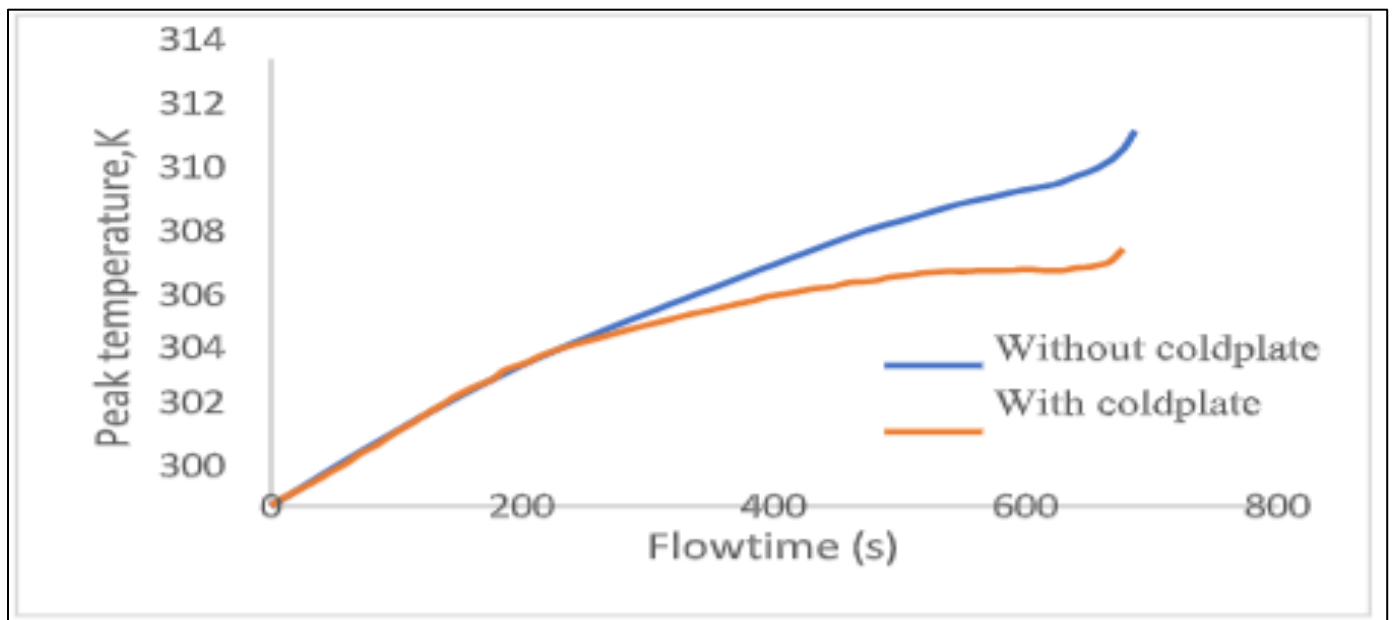


Fig 17 Variation of Peak Temperature of LIB Cell with MCP for 5C.

It is noted from the simulations that the temperature of cell increases with flow time at high discharge rates. Therefore, it is felt essential to employ thermal management with MCP with optimized parameters of MCP as presented above. Therefore, by employing MCP to manage the heating of the cell, the peak temperature of cell has been observed to be reduced effectively as depicted in Figure 17. From the predictions through simulations, the peak temperature of LIB with MCP at discharge rates of 3C and 5C respectively, are obtained, and for a mass flow rate of 5e-4 kg/s are, as shown in Figure 18[a] and [b].

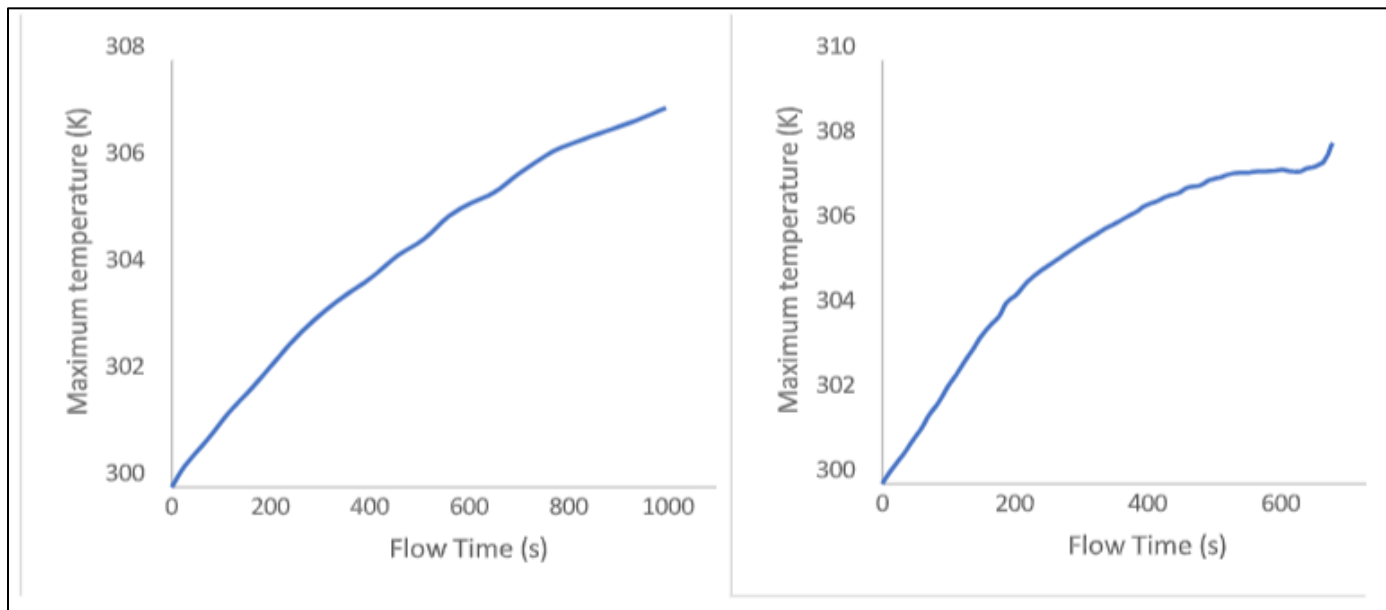


Fig 18[A]: Maximum Temperature of Lithium- Ion Cell with Mini-Channel Cold Plate during 3C Fig 18[B]: Maximum Temperature of Lithium-Ion Cell with Mini-Channel Coldplate during 5C

*D. Mini-Channel Cold Plates for the Effective Thermal Management of Lithium-Ion Battery Packs*

Considering the battery pack and at 5C discharge rate, simulations were performed for two different battery packs (Design 1, Design 2) with MCPs for different mass flow rates with straight, wavy, zig- zag channels.

➤ *Mini Channel Cold Plate for the Cooling Of Design 1 with Straight Channels*

As stated, each cell is inserted by two adjacent MCPs and denoted as Design-1. The simulation methodology is explained earlier. For design 1 at a 5C discharge rate and a mass flow rate of 5e-05 kg/s through straight mini-channels, the peak temperature in the battery pack with and without cold plates is compared to understand the effectiveness of cold plates. The simulations are done, and the temperatures obtained are shown in Figure 19. It can be seen that the peak temperature of the battery pack is dropped with cold plates.

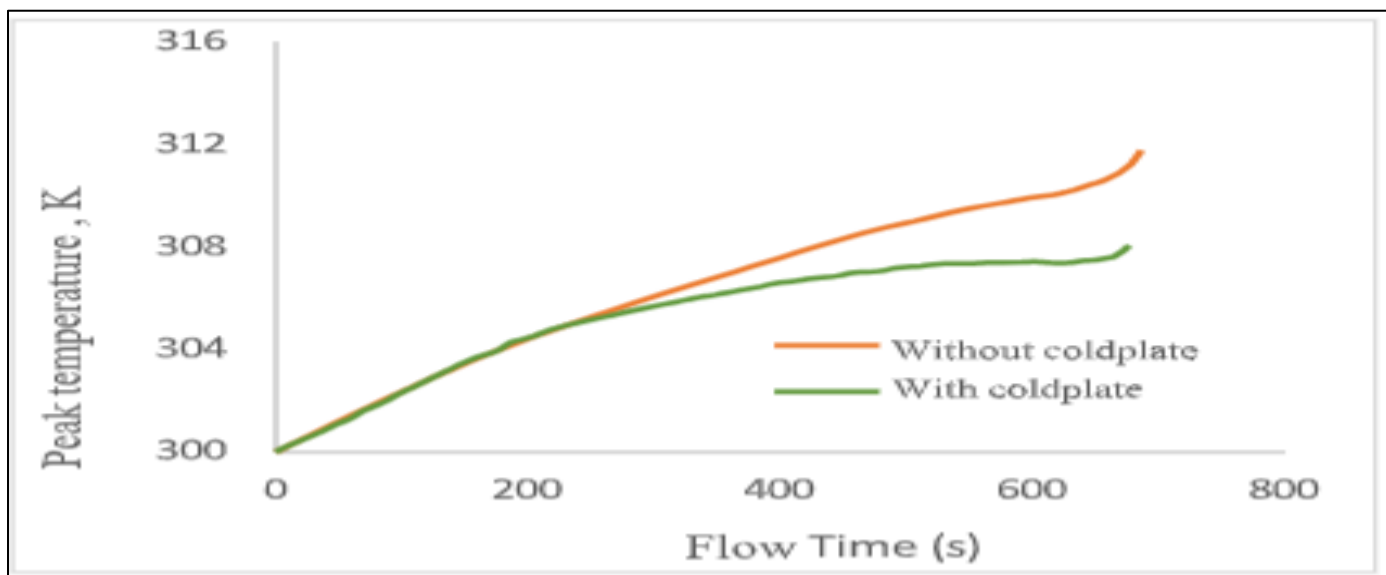


Fig 19 Battery Peak Temperature with and Without Cold Plate under Discharge 5C

➤ *Effect of Mass Flow Rate for Design 1 with Straight Channels*

The effect of mass flow rate is studied on the maximum temperature and pressure drop of coolant and it is observed that beyond flow rate of 5e-05 kg/s, there seen to be reduction in peak temperature but sharp rise in pressure drop

necessitating higher energy consumption and hence 5e-05 kg/s has been chosen as optimum flow rate and further simulations done with the optimized flow rate. The variation of maximum temperature and pressure drop with flow rate are shown in Figures 20[a] and 20[b] respectively.

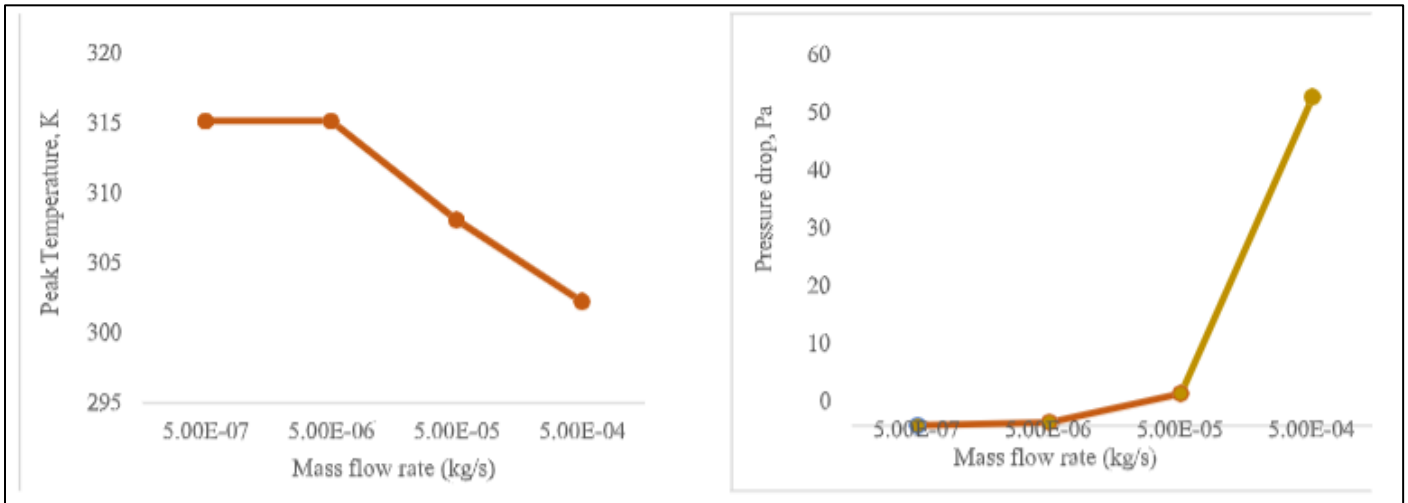


Fig 20 [A]: The Variation of Maximum Temperature with Mass Flow Rate Fig 20[B]: the Variation of Pressure Drop with Mass Flow Rate

➤ *Effect of number of channels for Design 1 with straight channels*

With flow rate of 5e-05 kg/s, further work on the effect of number of channels for cold plate was carried out by changing the number of channels as 4,8 and 10 without altering the cold plate geometry. Figure

4.21 illustrates the variation of the maximum temperature of the battery pack with a number of channels, and it can be observed that with an increase in a number of channels, the maximum temperature has decreased significantly, and it is concluded that for the chosen geometry, number of channels as 10 yielded lower battery temperature compared to lesser number of channels.

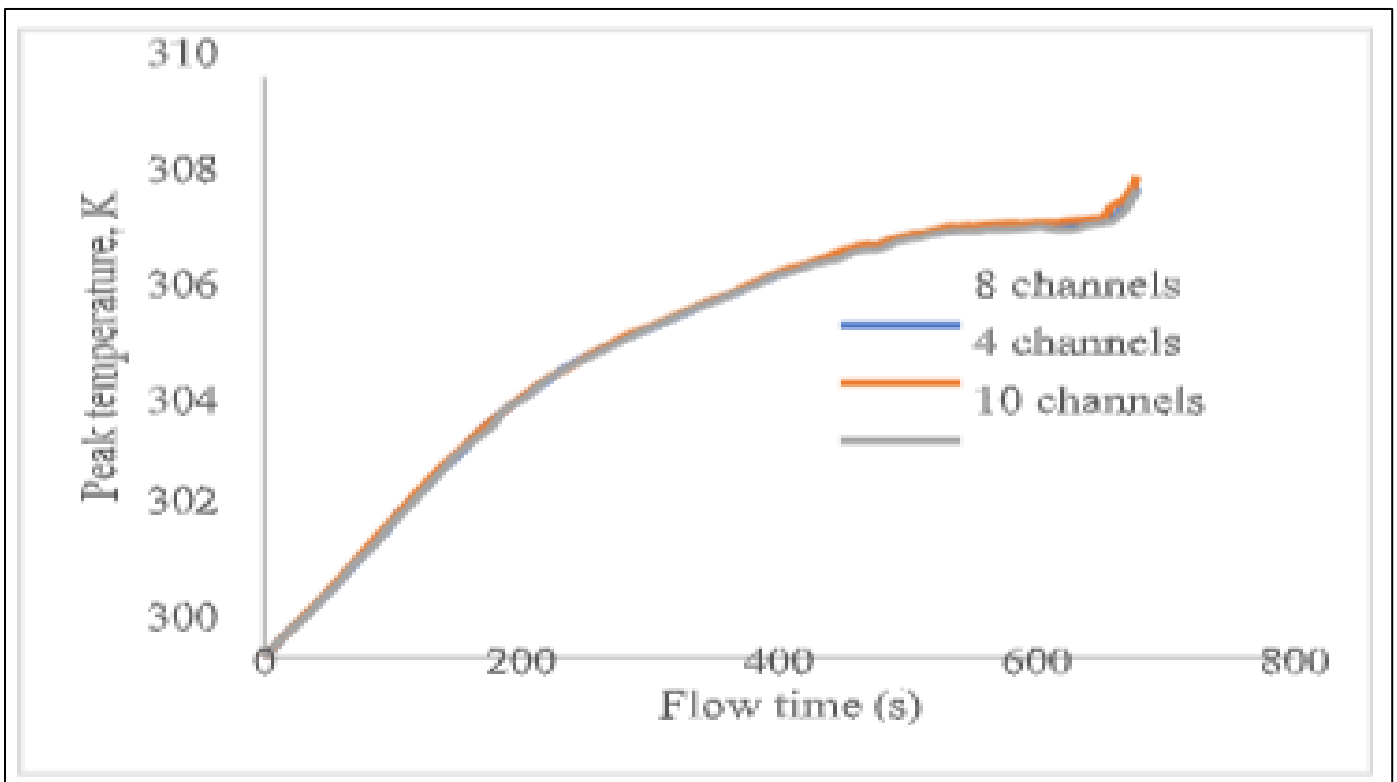


Fig 21 the Variation of Peak Temperature with Time for Number of Channels 4,8,10 Respectively.

➤ *Mini-Channel Cold Plates Design 1 with Wavy Channels*

Simulations has been done for design 1 with wavy for four different mass flow rates during discharge rate of 5C. For The same conditions of cross-sectional area, number of

Channels, discharge rate and mass flow rate, it is observed that the peak battery temperature has been decreased as shown in Figure 4.22.

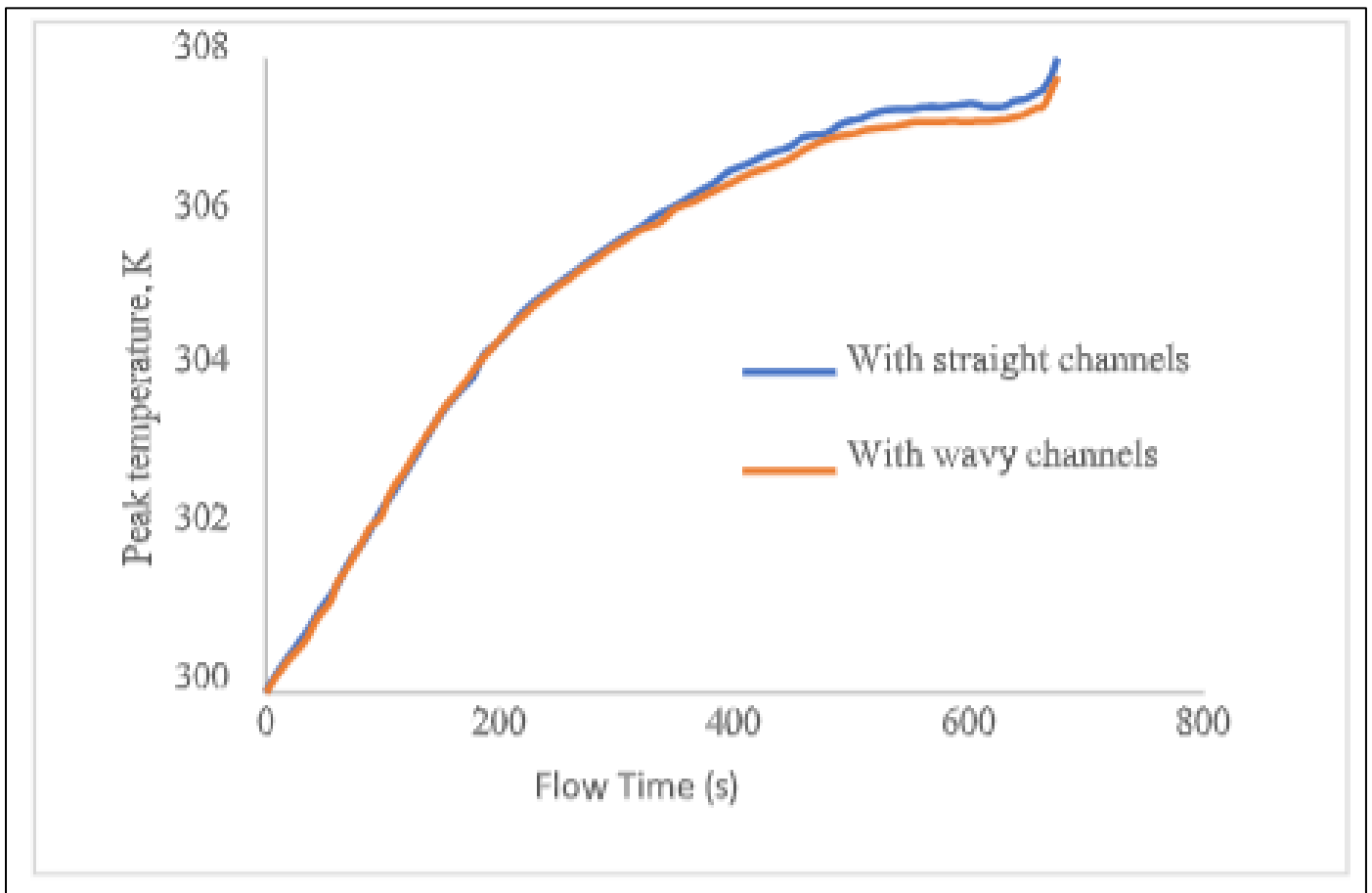


Fig 22 the Variation of Peak Temperature with Time for Straight and Wavy Channels at 5C.

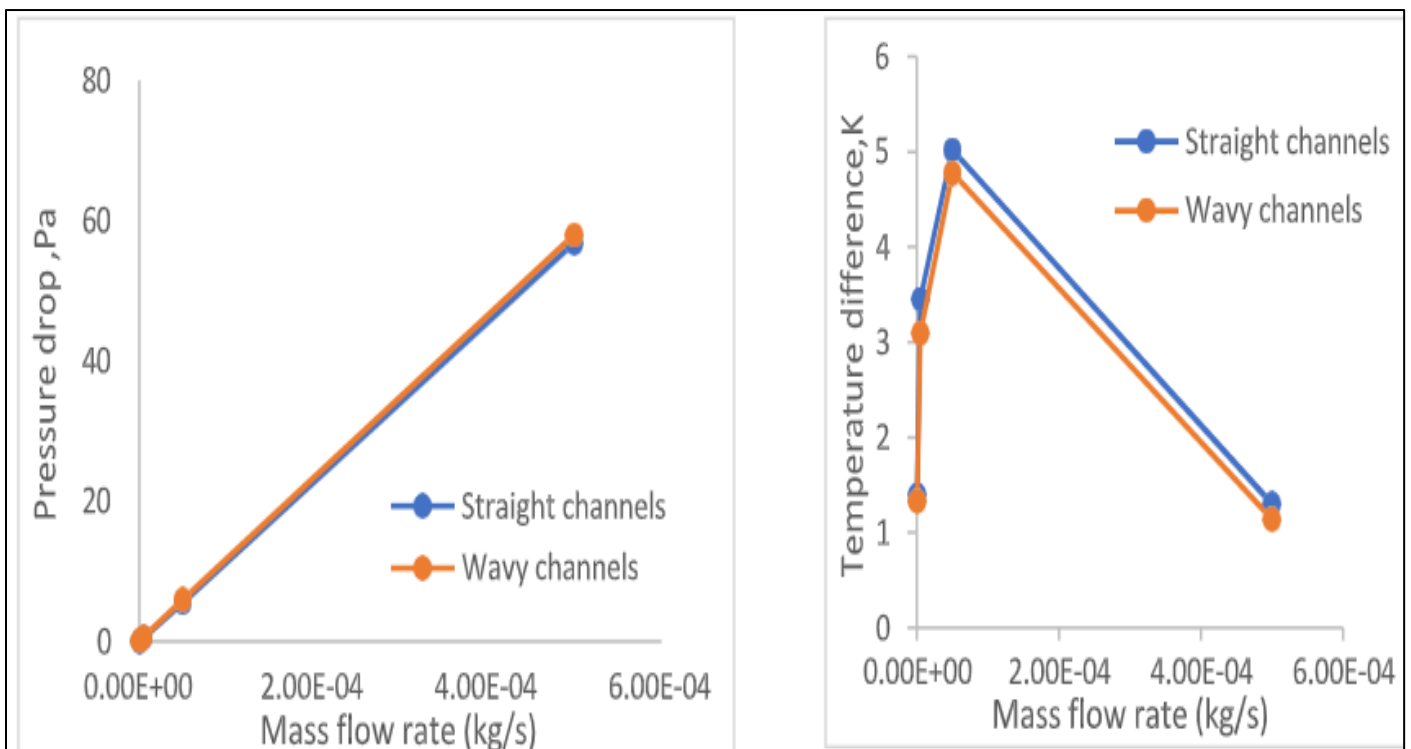


Fig 23 [A]: Variation of Pressure Drop with Mass Flow Rate. Fig 23[B]: Variation of Temperature Difference with Mass Flow Rate.

It is also observed that with wavy channels, there is a slight increase in pressure drop and temperature uniformity

also increasing as shown in Figures 23[a] and 23[b] respectively.

➤ *Mini Channel Cold Plates for Design 2 with Straight Channels*

Further simulations are carried out by keeping that every five cells are inserted between two MCPs and treating the case as Design-2. Again, the simulations are performed for the discharge rate of 5C with different mass flow rates of coolant, different number of channels, and different channel profiles like wavy and zig-zag.

➤ *Effect of Mass Flow Rate for the Cooling Of Design 2 with Straight Channels*

It is observed that with increase in mass flow rate the maximum temperature of battery is decreased whereas pressure drop is increasing as shown in Figures 24[a] and 24[b] respectively. It is also observed that increasing mass flow rate beyond  $5 \times 10^{-4}$  kg/s, there is a rapid increase in pressure drop.

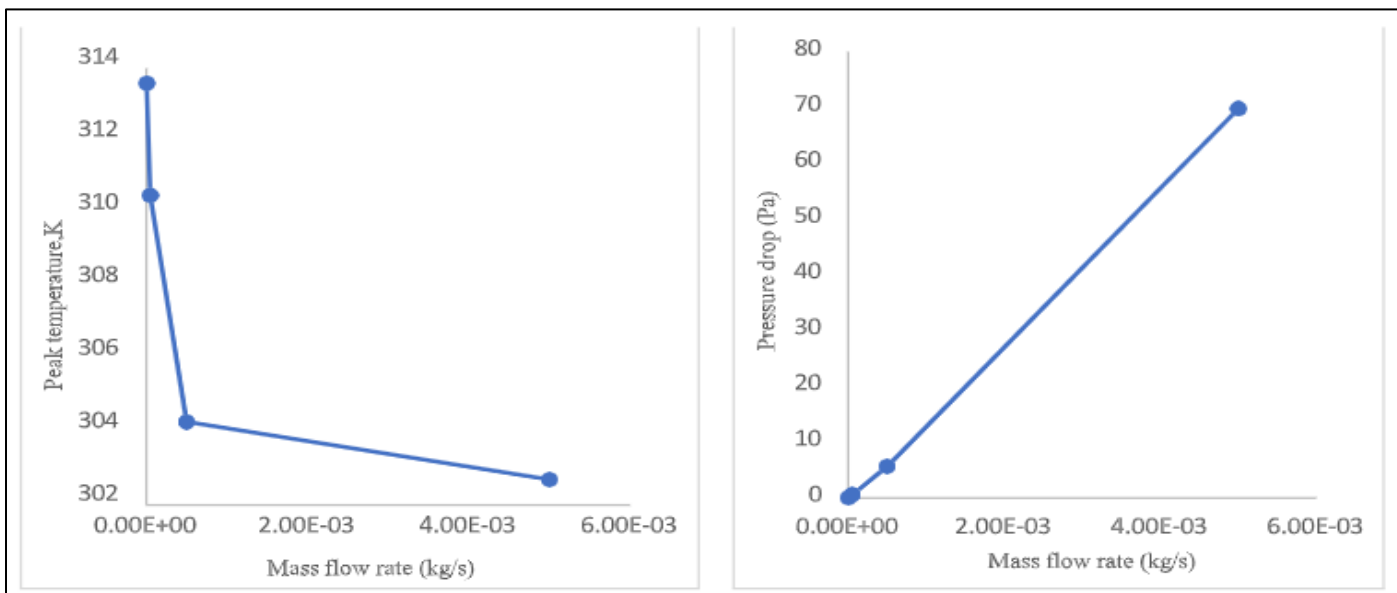


Fig 24[A]: Variation of Maximum Temperature with Mass Flow Rate      Fig 24[B]: Variation of Pressure Drop with Mass Flow Rate

In addition to peak temperature and pressure drop, temperature uniformity in the battery pack and in individual are very much needed for the thermal management. Figure 25[a] shows the temperature uniformity in cell 1 which is adjacent to cold plate with respect to mass flow rate and Figure 25[b] shows the temperature uniformity in the battery pack (that is temperature difference among cells) for a mass

flow rate of  $5 \times 10^{-4}$  kg/s. It is observed that except for the mass flow rate of  $5 \times 10^{-6}$  kg/s, which is very much low compared to all other mass flow rates, the temperature difference is less than 5 to an  $5^{\circ}\text{C}$ . It is also observed that the temperature difference between the cells adjacent to cold plate and the cells in middle of the battery pack is less than  $5^{\circ}\text{C}$ .

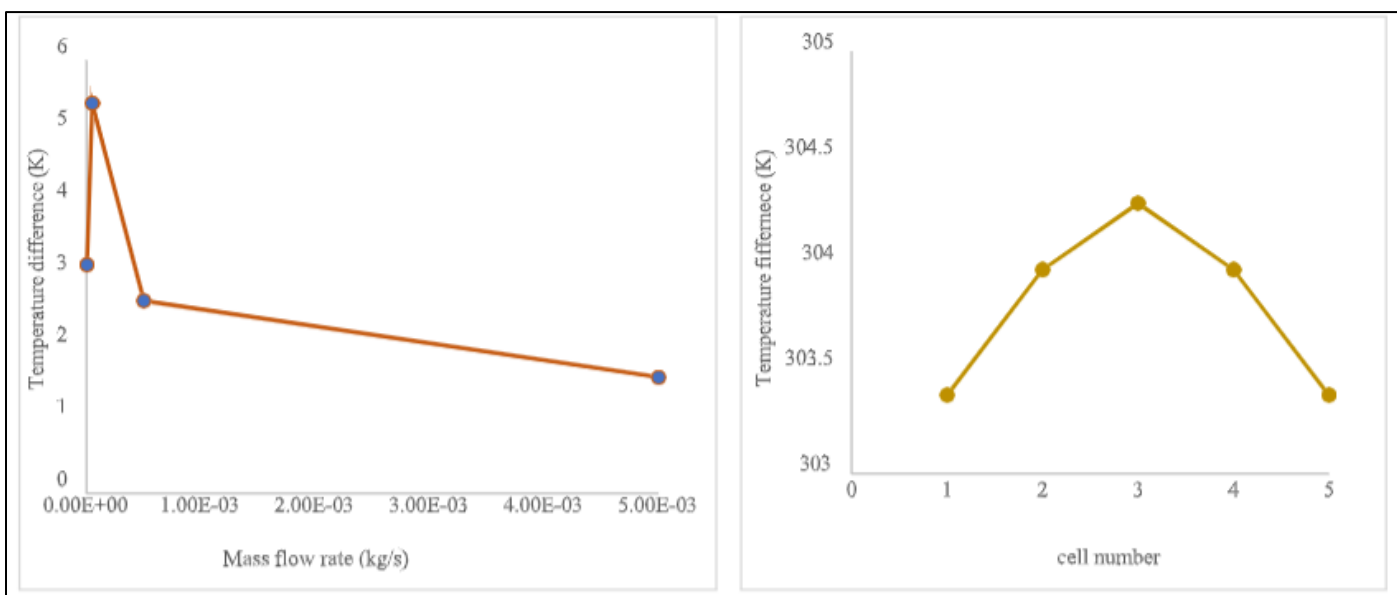


Fig 25[A]: Variation of Temperature Difference in A Cell with Mass Flow Rate      Fig 25[B]: Variation of Temperature Difference in A Battery Pack with Mass Flow Rate

➤ *Effect of Number of Channels for Design 2 with Wavy Channels*

Simulations have been done for four different mass flow rates for different numbers of channels for 4,8, and 10, as shown in Figure 26[a].

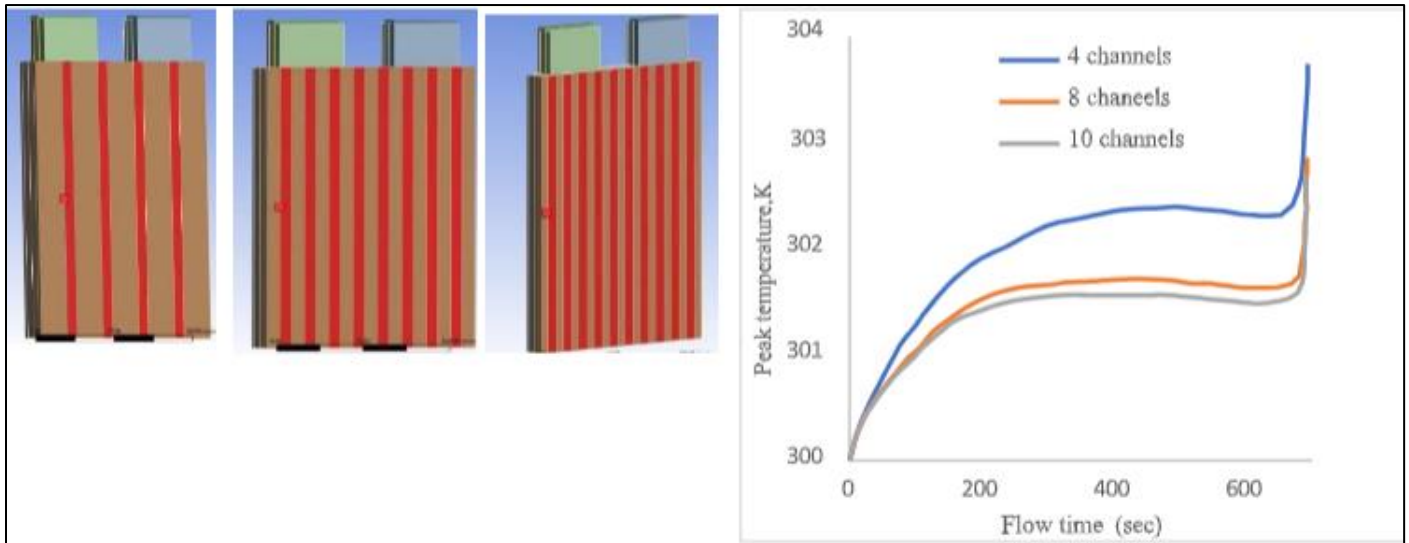


Fig 26[A]: Geometry of Design 2 with a Number of Channels of 4,8,10 Respectively [B]: Variation of Maximum Temperature with Flow Time for Different Number of Channels

It is observed that for same mass flow rate by increasing number of channels peak temperature of battery pack is decreasing as shown in Figure 26[b]. It is also observed that temperature uniformity is increasing and pressure drop is decreasing by increasing number of channels as shown in Figures 27[a] and 27[b] respectively.

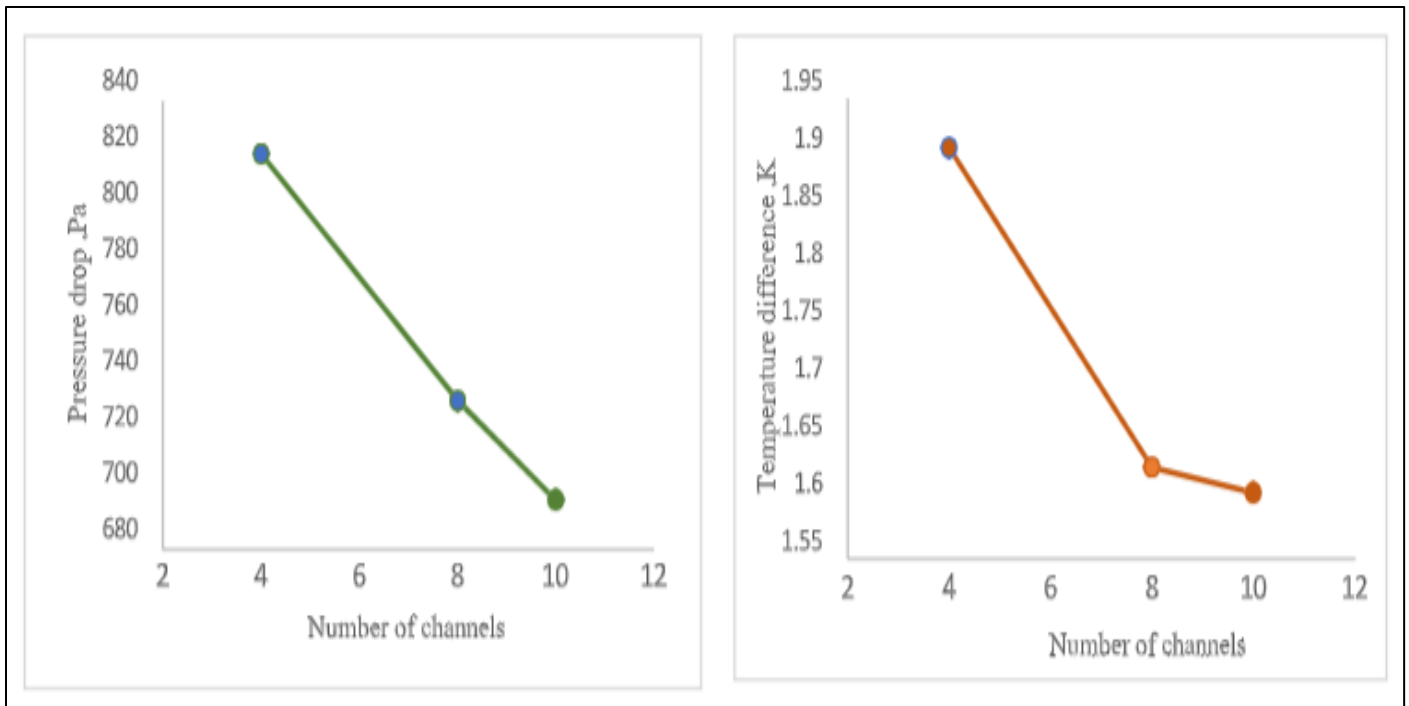


Fig 27[A]: Variation of Pressure Drop with Different Number of Channels 27 [B]: Variation of Temperature Difference with Different Number of Channels

➤ *Mini Channel Cold Plate for Design 2 with Straight and Wavy Channels*

Simulations are done for Design 2 with straight and wavy channels. From the simulation results, it was observed that the maximum temperature of the battery decreases with wavy channels, as shown in Figure 28[b].

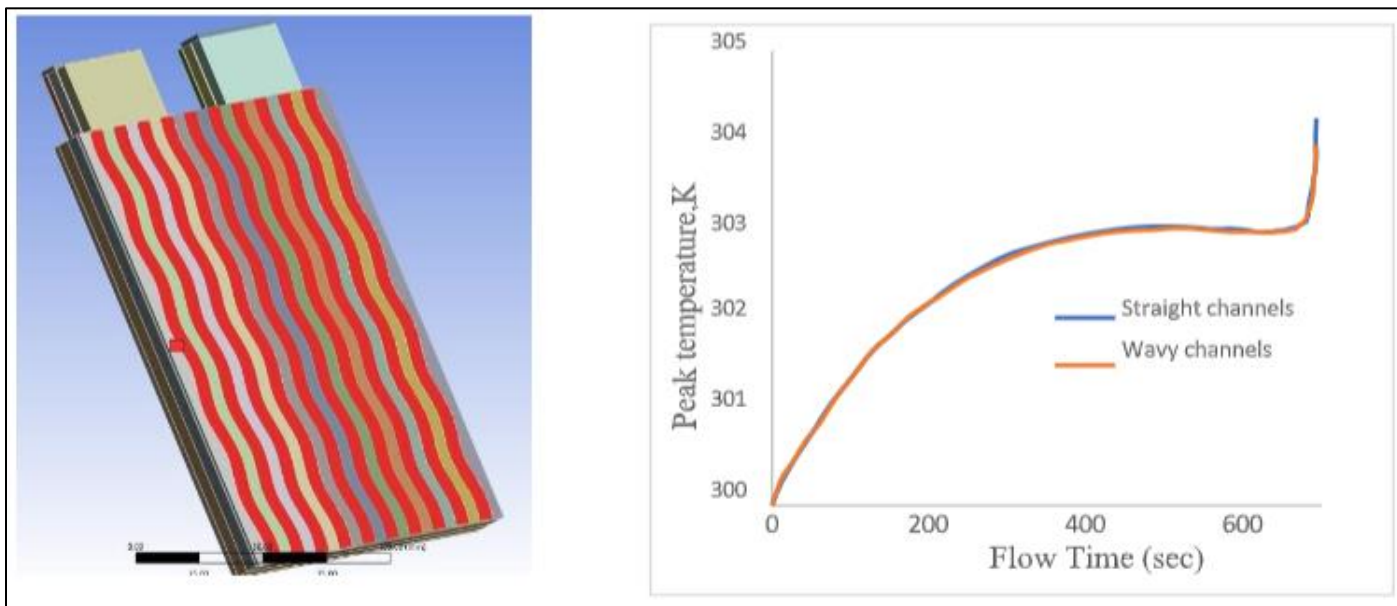


Fig 28[A]: Design 2 with Wavy Channels. Fig 28[B]: Variation of Peak Temperature with Flow Time for Straight and Wavy Channels.

It is also observed that temperature uniformity is increasing with wavy channels whereas pressure drop is increasing because of the constriction offered to the flow. The effect of wavy channels on temperature difference and pressure drop are shown in Figures 29[a] and 29[b] respectively.

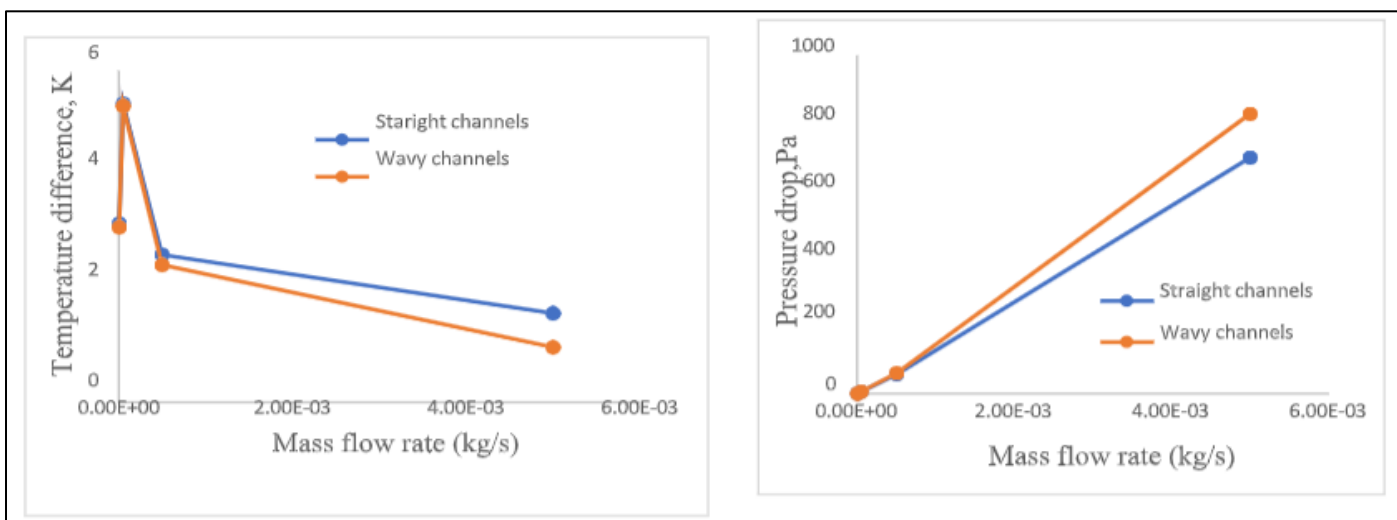


Fig 29[A]: Variation of Temperature Difference with Mass Flow Rate for Straight and Wavy Channels  
 Fig 29[B]: Variation of Pressure Drop with Mass Flow Rate for Straight and Wavy Channels

In addition, in order to know the effect of amplitude and wavelength, 6 different cases have been simulated and the results for a mass flow rate of  $5e-4$  kg/s are shown Table 3. It is observed that maximum temperature almost remained constant whereas pressure drop is varied significantly and is found to be highest when amplitude is equal to 1.5mm and wavelength is equal to 27.4mm.

Table 3 Variation of Maximum Temperature and Pressure Drop for Different Designs of Wavy Channels

Amplitude(A) and wavelength( $\lambda$ ) in mm	Maximum temperature, K	Pressure drop, Pa
A=1.5 mm, $\lambda$ = 38.4 mm	303.972 K	6.628 Pa
A=1 mm, $\lambda$ = 38.4 mm	303.979 K	6.370 Pa
A= 2 mm, $\lambda$ = 38.4 mm	303.964 K	7.125 Pa
A=1.5 mm, $\lambda$ = 27.4 mm	303.990 K	7.383 Pa
A= 1 mm, $\lambda$ =27.4 mm	303.984 K	6.643 Pa
A=2 mm, $\lambda$ = 27.4 mm	303.979 K	8.687 Pa

➤ *Mini Channel Cold Plate for Design 2 with Zig-Zag Channels*

From the simulation results it was observed that peak temperature of battery has marginally decreased with zig-zag channels compared to straight and wavy channels as shown in Figure 30[a].

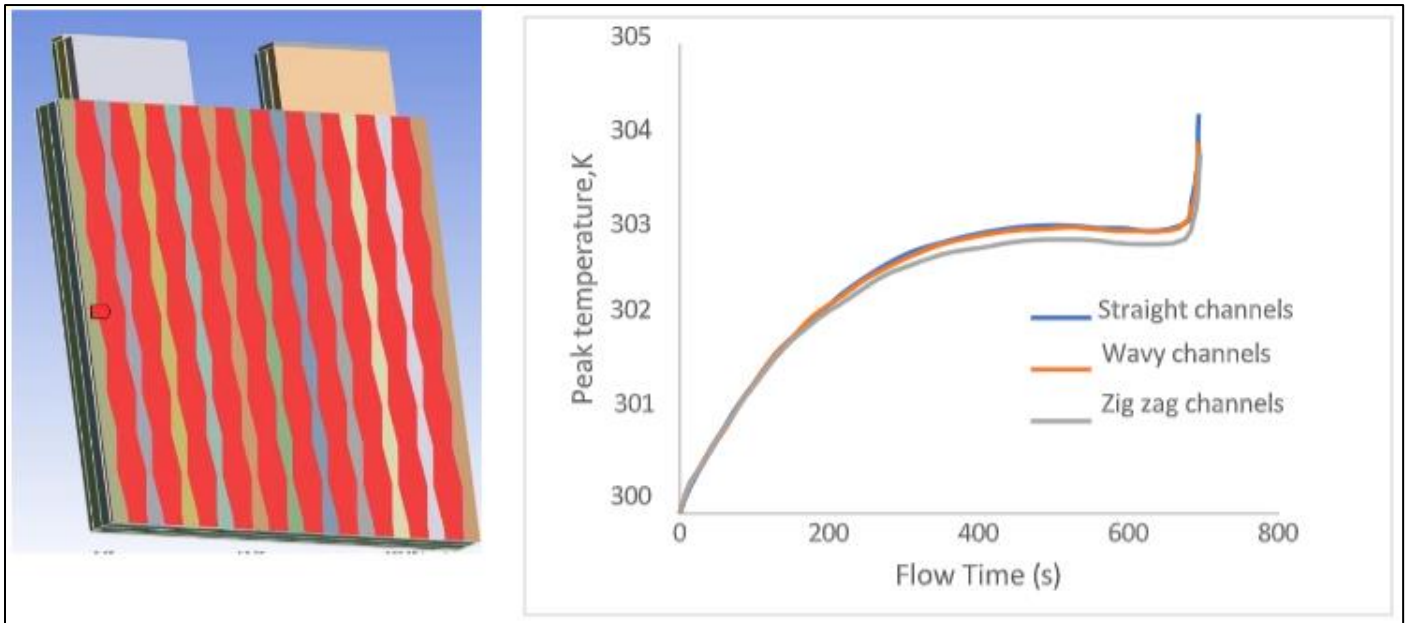


Fig 30[A]: Design 2 with Zig-Zag Channels Fig 30[B]: Variation of Peak Temperature with Flow Time for Straight, Wavy and Zig-Zag Channel

It is also observed that temperature uniformity is increasing, whereas pressure drop is also increasing because of the restriction offered to the flow of coolant. The effect of zig-zag channels on temperature difference and pressure drop is shown in Figures 31[a] and 31[b] respectively.

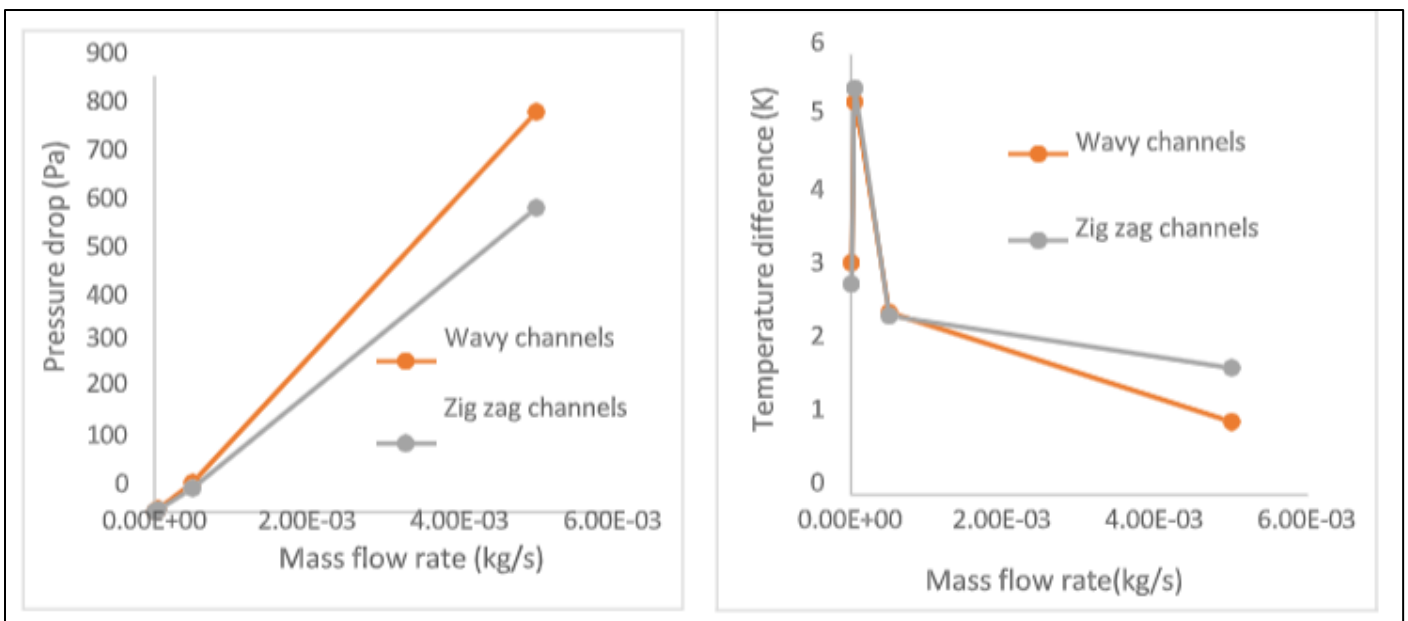


Fig 31[A]: Variation of Pressure Drop With Mass Flow Rate for Wavy and Zig-Zag Channels 31[B]: Variation of Temperature Difference with Mass Flow Rate for Wavy and Zig-Zag Channel

The lowest peak battery temperatures obtained with MCP for the two cases Design 1 and Design 2 are compared. Figure 32 illustrates the temperatures obtained with MCP for a discharge rate of 5C.

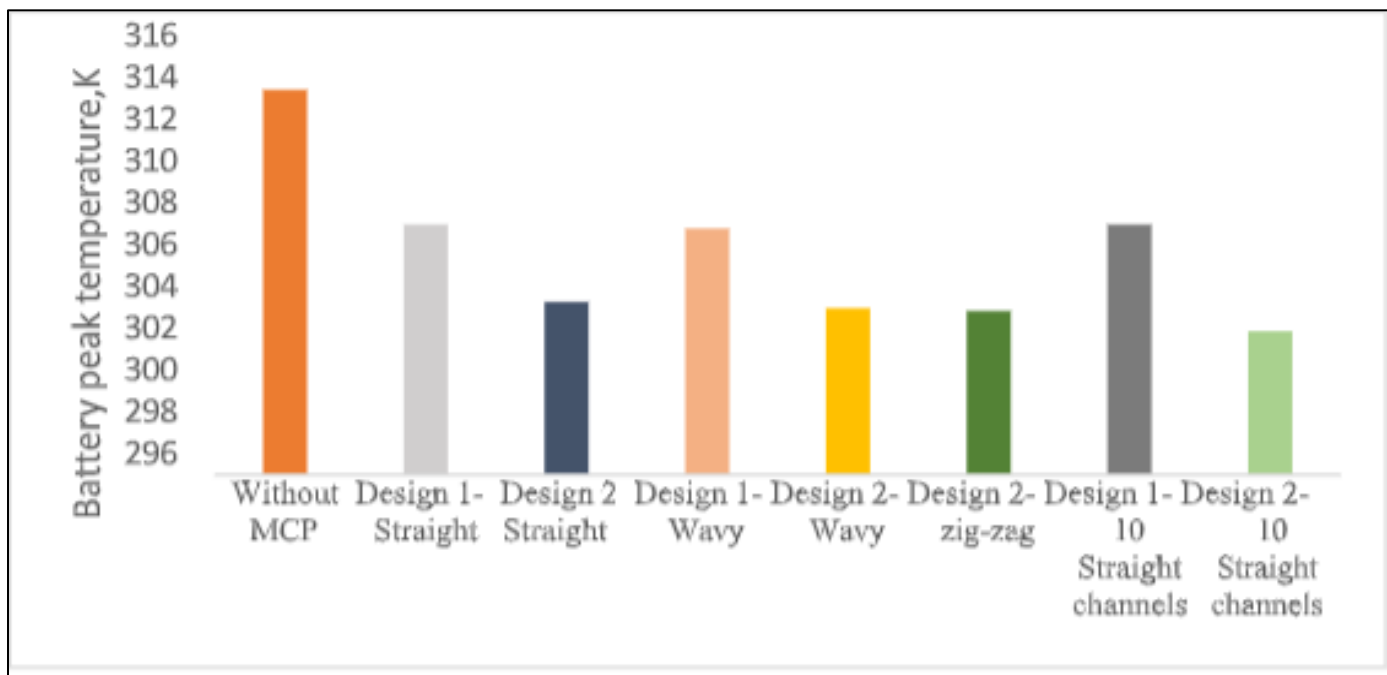


Fig 32 Comparison among Cases for Design 1 and Design 2 for a Discharge Rate 5C.

Though the temperature of Design 2 with zig-zag channels is marginally lower but considering practical difficulties in the fabrication of zig-zag channels and the values could be well within the experimental errors. Moreover, in Design 1, the MCP are inserted adjacent to every two cells, whereas in Design 2, two MCP are inserted for every five cells. Therefore, the cooling system of Design 1 is heavier than Design 2. In addition, as the number of channels are increased, the peak temperature reduced. However, for greater number of channels, 10 channels, the peak temperatures are 307.96 K and 302.86 K for Design 1 and Design 2 respectively. Hence, Design 2 exhibited the lowest peak temperature. Hence, it is concluded that Design 2 with ten number of straight channels could be preferred for the present configuration.

**V. CONCLUSION**

The chosen software well predicted the thermal behavior of a single cell and battery back for different conditions. Based on the numerical work on the chosen prismatic cell configuration with the use of MCP, the following conclusions are drawn.

Thermal management is essential for better and safe operation of LIBs especially at higher discharge rates.

By increasing mass flow rate and number of channels, peak temperature of battery is decreasing and temperature uniformity is improved.

Compared to straight and wavy channels, zig-zag channels yielded lower battery temperatures.

For the proposed battery packs with mini-channel cold plates, number of channels has more influence than changing the profiles to wavy and zig-zag.

Increasing the number of channels, changing the profiles to wavy and zig-zag has greater significance at high discharge rates.

Cross section of the straight channels has little influence on the performance of cold plate.

Between the two designs, Design 2 yielded better results of thermal management.

**ACKNOWLEDGEMENT**

The authors heartfully thank the authorities of NIT Warangal-India for providing computational facilities with access to licensed ANSYS FLUENT software R1 and a digital library for accessing journals of repute.

- *Conflict of Interest Statement*  
The authors declare no conflict of interest.
- *Data Availability Statement*  
The data reported in this manuscript are available from the corresponding author upon reasonable request.
- *Funding*  
No funding from external agencies is utilized.

**REFERENCES**

[1]. John B. Heywood Internal Combustion Engines Fundamental Mc Graw Hill Co. 2018  
 [2]. Rao, G.A.P, Sharma,T.K,2020, Engine Emission Control Technologies-Design Modifications and Pollution Mitigation Techniques, 1st Edition Apple Academic Press-CRC, Taylor & Francis Group, New York.

- [3]. Larminie James, *Electric vehicle technology explained* John Wiley, 2012.
- [4]. Shahjalal, M., Shams, T., Islam, M. E., Alam, W., Modak, M., Hossain, S.B., Ramadesigan, V., Ahmed, M. R., Ahmed, H., & Iqbal, A. (2021) 'A review of thermal management for Li-ion batteries: Prospects, challenges, and issues', *Journal of Energy Storage*, Vol.39. 102518.
- [5]. Wang, Q., Mao, B., Stoliarov S.I., Sun, J., 2019, A review of lithium ion battery failure mechanisms and fire prevention strategies, *Progress in Energy and Combustion Science*, 73, pp.95-131.
- [6]. Chawla, N.; Bharti, N.; Singh, S. (2019) 'Recent Advances in Non-Flammable Electrolytes for Safer Lithium-Ion Batteries', *Batteries*, Vol.5(1), 19.
- [7]. Vadim F. Yakovlev, V.F. (2022) 'Early electric vehicle charging: a survey', *International Journal of Electric and Hybrid Vehicles*, Vol. 14(3), pp.219–230.
- [8]. Arvind, S. P., Soni, B.P., Kishor V. Bhadane, K.V. (2023) 'Classification and review of electric circuit models for electric vehicle batteries', *International Journal of Electric and Hybrid Vehicles*, Vol. 15 (2), pp. 107–126.
- [9]. Sivakrishnamraju Rallabandi, Rajay Vedaraj Issac Selvaraj *Advancements in Battery Cooling Techniques for Enhanced Performance and Safety in Electric Vehicles: A Comprehensive Review*, *Energy Technology*, Wiley, 2024, <https://doi.org/10.1002/ente.202301404>.
- [10]. Foo Shen Hwang, Thomas Confrey, Colin Reidy, Dorel Picovici, Dean Callaghan, David Culliton, Cathal Nolan *Review of battery thermal management systems in electric vehicles* *Renewable and Sustainable Energy Reviews* 192 (2024) 114171.
- [11]. A.G. Olabi, Hussein M. Maghrabie, Ohood Hameed Kadhim Adhari, Enas Taha Sayed, Bashria A.A. Yousef, Tareq Salameh, Mohammed Kamil, Mohammad Ali Abdelkareem *Battery thermal management systems: Recent progress and challenges* *International Journal of Thermofluids*, Vol.15, 2022, 100171
- [12]. Mali, V., Saxena, R., Kumar, K., Kalam, A., Tripathi, B. (2021) 'Review on battery thermal management systems for energy-efficient electric vehicles', *Renewable and Sustainable Energy Reviews*, Vol. 151.
- [13]. Feng, X., Xu, C., He, X., Wang, L., Zhang, G., Ouyang, M. (2018) 'Mechanisms for the evolution of cell variations within a LiNixCoyMnzO2/graphite lithium-ion battery pack caused by temperature non-uniformity', *Journal of Cleaner Production*, Vol.205, pp.447462.
- [14]. Yue, Q. L., He, C. X., Wu, M. C., Zhao, T. S. (2021) 'Advances in thermal management systems for next-generation power batteries', *International Journal of Heat and Mass Transfer*, Vol. 18.
- [15]. Tete, P. R., Gupta, M. M., & Joshi, S. S. (2021) 'Developments in battery thermal management systems for electric vehicles: A technical review', *Journal of Energy Storage*, Vol. 35.
- [16]. Patel, J. R., Rathod, M. K. (2020) 'Recent developments in the passive and hybrid thermal management techniques of lithium-ion batteries', *Journal of Power Sources*, Vol.480.
- [17]. Murali. G., G.S.N. Sravya, J. Jaya, V. Naga Vamsi *A review on hybrid thermal management of battery packs and its cooling performance by enhanced PCM* *Renewable and Sustainable Energy Reviews* Volume 150, 2021, 111513.
- [18]. Sheu, S. P., Yao, C. Y., Chen, J. M., Chiou, Y. C. (1997) 'Influence of the LiCoO2 particle size on the performance of lithium-ion batteries', *Journal of Power Sources*, Vol. 68.
- [19]. Jarrett, A., Kim, I. Y. (2011) 'Design optimization of electric vehicle battery cooling plates for thermal performance', *Journal of Power Sources*, Vol.196 (23), pp.10359–10368.
- [20]. Huo, Y., Rao, Z., Liu, X., and Zhao, J. (2015) 'Investigation of power battery thermal management by using mini-channel cold plate', *Energy Conversion and Management*, Vol. 89, pp.387–395.
- [21]. Qian, Z., Li, Y., and Rao, Z. (2016) 'Thermal performance of lithium-ion battery thermal management system by using mini-channel cooling', *Energy Conversion and Management*, Vol.126, pp.622–631.
- [22]. Panchal, S., Khasow, R., Dincer, I., Agelin-Chaab, M., Fraser, R., and Fowler, M. (2017) 'Thermal design and simulation of mini-channel cold plate for water cooled large sized prismatic lithium-ion battery', *Applied Thermal Engineering*, Vol.122, pp. 80–90.
- [23]. Deng, T., Zhang, G., and Ran, Y. (2018) 'Study on thermal management of rectangular Li-ion battery with serpentine-channel cold plate', *International Journal of Heat and Mass Transfer*, Vol.125, 143–152.
- [24]. Liu, H., Chika, E., and Zhao, J. (2018) 'Investigation into the effectiveness of nanofluids on the mini-channel thermal management for high power lithium-ion battery', *Applied Thermal Engineering*, Vol. 142, pp. 511–523.
- [25]. Sheng, L., Su, L., Zhang, H., Li, K., Fang, Y., Ye, W., and Fang, Y. (2019) 'Numerical investigation on a lithium ion battery thermal management utilizing a serpentine-channel liquid cooling plate exchanger', *International Journal of Heat and Mass Transfer*, Vol.141, pp.658–668.
- [26]. Deng, T., Zhang, G., Ran, Y., and Liu, P. (2019) 'Thermal performance of lithium-ion battery pack by using cold plate', *Applied Thermal Engineering*, Vol. 160.
- [27]. Huang, Y., Mei, P., Lu, Y., Huang, R., Yu, X., Chen, Z., and Roskilly, A. P. (2019) 'A novel approach for Lithium-ion battery thermal management with streamline shape mini-channel cooling plates', *Applied Thermal Engineering*, Vol. 157.
- [28]. Liu, H. ling, Shi, H. bo, Shen, H., and Xie, G. (2019) 'The performance management of a Li-ion battery by using tree-like mini-channel heat sinks: Experimental and numerical optimization', *Energy*, Vol. 189.

- [29]. Amalesh, T., Narasimhan, N. L. (2020) 'Introducing new designs of mini- channel cold plates for the cooling of Lithium-ion batteries', *Journal of Power Sources*, Vol.479, 228775.
- [30]. Zuo, S., Chen, S., & Yin, B. (2022). Performance analysis and improvement of lithium-ion battery thermal management system using mini-channel cold plate under vibration environment. *International Journal of Heat and Mass Transfer*, 193. <https://doi.org/10.1016/j.ijheatmasstransfer.2022.122956>
- [31]. Madaka Ramu Mini-channel cold plates for the effective thermal management of Lithium-Ion batteries M.Tech dissertation submitted to NIT Warangal 2023.
- [32]. Ugur Morali A numerical and statistical implementation of a thermal model for a lithium-ion battery *Energy*240 (2022) 122486.